Distribution Agreement

In presenting this thesis or dissertation as a partial fulfillment of the requirements for an advanced degree from Emory University, I hereby grant to Emory University and its agents the non-exclusive license to archive, make accessible, and display my thesis or dissertation in whole or in part in all forms of media, now or hereafter known, including display on the world wide web. I understand that I may select some access restrictions as part of the online submission of this thesis or dissertation. I retain all ownership rights to the copyright of the thesis or dissertation. I also retain the right to use in future works (such as articles or books) all or part of this thesis or dissertation.

Signature:

_____ _____

Nyasia M Jones Date

Mechanisms of Nodular and Infiltrative Pattern of Uveal Melanoma in the Liver

By

Nyasia M Jones, BS

Master of Science

Graduate Division of Biological and Biomedical Sciences
Cancer Biology and Translational Oncology

_____
Advisor: Hans E. Grossniklaus, MD, MBA

_____
Committee Member: Erwin G. Van Meir, PhD

_____
Committee Member: David H. Lawson, MD

Accepted:

_____

Lisa A. Tedesco, Ph.D.
Dean of the James T. Laney School of Graduate Studies

_____

Date

Mechanisms of Nodular and Infiltrative Pattern of Uveal Melanoma in the Liver

By

Nyasia Jones, BS

Advisor: Hans E. Grossniklaus, MD, MBA

An abstract of

A thesis to the Faculty of the James T. Laney School of Graduate Studies of Emory University in partial fulfillment of the requirements for the degree of Master of Science, Cancer Biology

2016

Abstract

Mechanisms of Nodular and Infiltrative Pattern of Uveal Melanoma in the Liver

By Nyasia Jones

The goal of this research is to gain more insight into the mechanisms by which uveal melanoma (UM) metastasizes to the liver and use this understanding to identify potential targets for therapy. There are two different metastatic growth patterns in the liver: the nodular pattern in which tumor cells surround the portal triad and the infiltrative pattern in which tumor cells invade the sinusoidal space. Pigment epithelium derived factor (PEDF) and natural killer (NK) cells have been implicated by previous research as protective mechanisms against progression of metastatic disease. NK cell depletion in a murine model of UM increased the number of hepatic metastases. Likewise, implanting murine melanoma cells in the uvea of PEDF KO mice resulted in dramatically larger angiogenic metastatic foci. Based on these observations, we hypothesized that knock out of PEDF would result in predominantly nodular pattern while depletion of NK cells would result in the infiltrative pattern of growth predominating. The wild-type model would have equal distribution of both patterns. To test this, we developed three murine models of uveal melanoma in mice with C57BL/6 background that form hepatic metastases: a NK cell deficient model using anti-asialo GM1 antibody, a PEDF KO model, and a model in wild-type mice. The right eyes of mice were inoculated with B16LS9 melanoma cells and at 7 days the eyes were enucleated. Three weeks later, the mice were euthanized and livers were routinely processed for histological evaluation. PEDF KO mice showed increased nodular to infiltrative pattern in comparison to wild type and NK cell deficient mice. Interestingly, NK cell deficient mice did not show increased infiltrative pattern, however NK cell deficiency resulted in significant increase in the number of hepatic metastases and significant increase in stage 2 nodular and infiltrative metastases. Finally, we investigated how loss of the protective functions of PEDF and NK cells affected infiltration of host protective immune cells in the liver. FACS data evidenced an increase in myeloid derived suppressor cells (MDSCs) and tumor associated dendritic cells, suggesting that NK cell or PEDF loss promote an immunosuppressed tumor microenvironment that facilitates tumor growth.

Mechanisms of Nodular and Infiltrative Pattern of Uveal Melanoma in the Liver

By

Nyasia Jones, BS

Advisor: Hans E. Grossniklaus, MD, MBA

A thesis to the Faculty of the James T. Laney School of Graduate Studies of Emory University in partial fulfillment of the requirements for the degree of Master of Science, Cancer Biology

2016

Acknowledgements

I would first like to thank Dr. Grossniklaus for accepting me into his lab although I had limited research experience. Thank you for being both a mentor and source of personal inspiration. I entered this program unsure of whether I wanted to pursue a career in research or attend medical school. Dr. Grossniklaus showed me that I can be a physician and also incorporate my interests in research into my future ventures. Dr. Grossniklaus' breadth of knowledge and passion for the field, have truly inspired me. He will always be a person I admire. Thank you, Dr. G, thesis would not have been possible without your continued support and faith in me.

Thank you Dr. Hua Yang for guiding me through much of this project, training me, and providing your expertise. I would like to thank Dr. Caroline Craven, and Jamie Story for your guidance and encouragement. To Micah Chrenek and Jana Sellers thank you for training me on various techniques, and for your patience. Also thank you to Vanessa Morales at the University of Tennessee for collaborating with me on this project. I am grateful for the guidance from my committee members Dr. Erwin Van Meir, and Dr. David Lawson. Thank you for your time and wisdom. I would like to thank Dr. Orloff for his mentorship and guidance throughout the program. A huge thanks to the Cancer Biology Graduate Program leadership who pioneered the creation of this new program, and gave me an immeasurable opportunity.

Lastly, I would like to thank my family and friends who were an endless source of encouragement and emotional support. Special thanks to my mother Nikisha Sanders and grandmother Elizabeth Jones who keep me mentally and spiritually grounded. To Chris, Jasmine, and Deana –I will forever be grateful for your support. Finally, to my great-grandmother Carmen Sanders, you will always be my source of strength.

Table of Contents

List of Figures

Introduction

Epidemiology of Uveal Melanoma

Uveal Melanoma is the most common form of malignant intraocular tumor in adults (Woll et al. 1999, Miyamoto et al. 2012). Uveal melanoma typically arises in the choroid, ciliary body, or iris, with 80% of neoplasms manifesting in the choroid (Figure 1)(Miyamoto et al. 2012). Uveal melanoma is considered a distinct entity compared to cutaneous melanoma, with 5% of all melanomas occurring in the eye (Albert et al. 1996, Woll et al. 1999). Uveal melanoma has a worse overall prognosis in comparison to cutaneous melanoma with a 15-year survival rate of 53% compared to 95% for cutaneous melanoma(Woll et al. 1999, McKinnon et al. 2003). Caucasians have an 8 times greater risk of disease than African Americans and three times greater risk than Asians. The causal role of UV radiation in disease is debated as the incidence of uveal melanoma has not increased during the last 40 years in comparison to cutaneous melanoma, and there is not a higher incidence of tumorigenesis in more light exposed areas of the eye (Woll et al. 1999). Uveal melanoma kills about half of those diagnosed; most succumbing to metastatic disease (Eagle 2013). The liver is the main site of metastasis; about 71% of patients with uveal melanoma develop liver metastases as the first or secondary site of metastasis (Woll et al. 1999, Eagle 2013). The mortality rate of patients with uveal melanoma has not significantly changed since 1973 due to the lack of an effective clinical treatment for metastatic disease (Miyamoto et al. 2012).

The Biology of the Primary Tumor

Uveal melanoma is a malignant neoplasm derived from uveal melanocytes

(Eagle 2013). The human eye consists of 3 layers: the cornea and sclera, the retina, and the uveal tract. The uveal tract is highly vascularized and is composed of three topographic sites: the iris, the ciliary body, and the choroid. Uveal melanocytes are neural crest derived cells located in the uveal tract (Hu et al. 2008). Benign nevi and malignant melanomas are derived from the uveal melanocytes and can arise in the iris, ciliary body, or choroid (**Figure 1**). The choroid is the most common site of neoplasm growth (80%), followed by the ciliary body (10%), and iris (10%)(Miyamoto et al. 2012). The melanocytes are a source of melanin, which is thought to be protective against several ocular diseases. Melanin in the uveal tract, more specifically the choroid and ciliary body, protects uveal melanocytes from oxidative stress and malignant transformation. UV radiation and biochemical activity produce reactive oxygen species, which can induce malignant transformation of uveal melanocytes (Hu et al. 2008) .

The choroid itself is highly vascularized, and the tumor choroid interface is essential in tumor development and vascularization. It is hypothesized that the tumor in the choroid co-opts off the mature vessels allowing tumor cells to receive oxygen and nutrients. Co-option of the mature choroidal vascular network feeds the initial neoplasm at its margins until the tumor is able to develop its own vasculature (Pina et al. 2009). Uveal melanoma typically presents as a dome shaped or nodular mass that forms into a mushroom-like protrusion due to the tumor rupturing the Bruch membrane (Miyamoto et al. 2012, Eagle 2013).

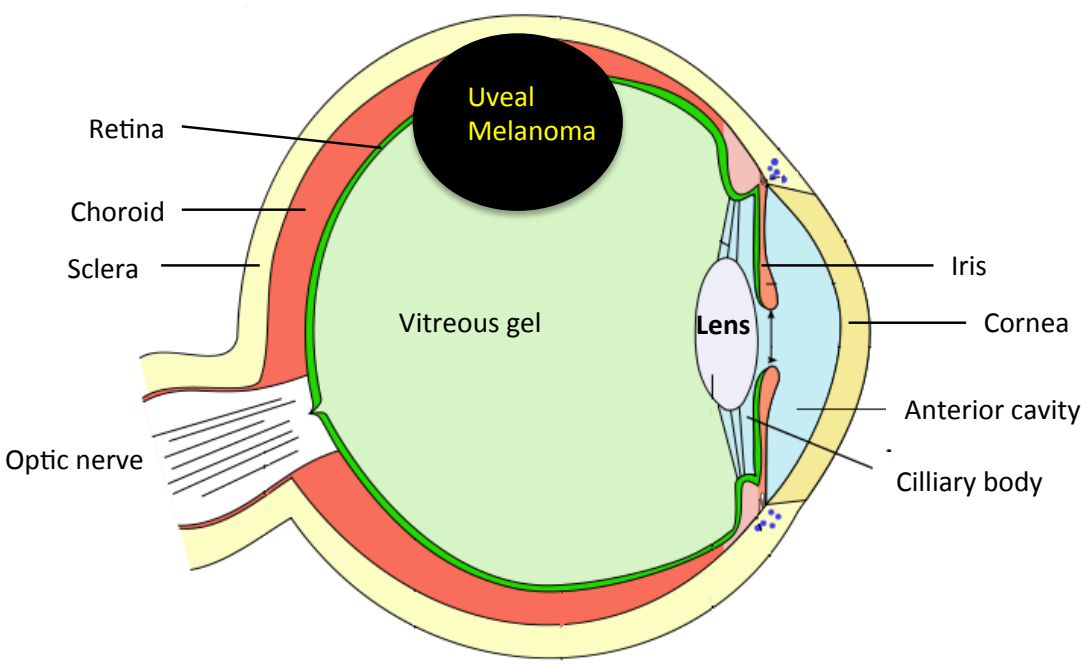

Figure 1 Uveal Melanoma in the Eye. Three layers compose the human eye: the cornea and sclera, the retina, and the uveal tract. The uveal tract is further composed of iris, ciliary body, and choroid. Uveal melanocytes within the uveal tract protect the eye from oxidative damage through the production of melanin. Uveal melanomas are derived from these melanocytes and lesions can arise in the choroid, ciliary body, or iris (Hu et al. 2008).

Diagnosis, Treatment, and Prognosis

Patients with uveal melanoma may present with symptoms such as blurred vision, metamorphopsia, visual field loss, flashes, or pain. However, a significant number of patients are asymptomatic and disease is detected during routine examination (Materin 2011, Miyamoto et al. 2012). Patients are clinically assessed by indirect opthlamoscopy, fundus photography, ultrasonography, and biopsy. Treatment options for uveal melanoma include surgical excision or enucleation, brachytherapy, and proton beam therapy (Materin 2011, Damato and Damato 2012). Treatment is usually dependent on tumor size, location, and the extent of disease. Early diagnosis and treatment may increase chances of vision conservation (Damato and Damato 2012). The first choice of treatment is usually brachytherapy with either iodine-125 or ruthenium-106 plaque (Materin 2011). However, about 20% of patients require enucleation as the primary treatment or following unsuccessful brachytherapy (Damato and Damato 2012). Despite advances in treatment, the 5-year survival rate of patients remained steady at 80% over a 35 year period (Singh et al. 2011).

Clinical and pathological factors are important in determining patient prognosis including: nucleoli size, tumor size, mitotic activity, tumor-infiltrating lymphocytes, age, and vascular patterns (Miyamoto et al. 2012). A worse prognosis is correlated with tumor size and invasion, invasion of sclera and/or optic nerve, and presence of an orange pigment. The location of the tumor is also important; patients with lesions in the choroid or ciliary body have a 54% 15-year survival rate, while patients presenting with lesions in the iris have a much better prognosis with

a mortality of less than 4% (Woll et al. 1999). An increased number of tumor infiltrating lymphocytes such as B- and T-lymphocytes are correlated with decreased survival (de la Cruz PO Jr., Miyamoto). Based on these prognostic factors, researchers developed a computerized system for determining patient prognosis from histological slides using multivariate analysis. Gamal and associates found that 13 variables strongly correlated with malignant potential and patient mortality (Gamel et al. 1982)

Uveal melanomas can be further classified by gene expression profiling (GEP) into class 1 and class 2 melanomas, in which class 1 patients have a lower risk of metastasis than class 2 (Harbour et al. 2010). Class 2 tumors have more than a 90% risk of metastasis in comparison to class 1 at less than 5% (Eagle 2013). The gene expression profile of class 1 melanomas resembles that of melanocytes while class 2 melanomas resemble primitive neural or ectodermal stem cells (Materin 2011, Eagle 2013). Furthermore, class 2 tumors show increased genomic instability and chromosomal abnormalities such as monosomy 3 (Eagle 2013). Monosomy 3 is an important predictor of survival, as it confers greater metastatic potential and rapidly progressive disease (**Figure 2**) (Abdel-Rahman et al. 2012). Tumors with loss of chromosome 3 contain a greater number of chromosomal abnormalities, and gain of metastatic competence (Landreville et al. 2008). Loss of chromosome 3 is also strongly correlated with inactivating somatic mutations of the gene encoding BAP1 (BRCA1- associated protein 1). The BAP1 gene is located at chromosome 3p21. BAP1 mutations coincide with the onset of metastatic progression and have been implicated as a key factor of metastatic competence and as a potential

therapeutic target (Harbour et al. 2010).

Additional studies of uveal melanoma have identified activating mutations in GNAQ or GNA11 that appear to occur early in tumor development (**Figure 2**) (Van Raamsdonk et al. 2009). Both GNAQ and GNA11 encode the G protein alpha-subunit, Gαq, which is a member of the q class of G proteins alpha-subunits involved in mediating downstream signaling in the RAF/MEK/ERK pathway (Eagle 2013, Xu et al. 2014). Mutations in GNAQ or GNA11 result in constitutively active G-protein due to decreased GTP hydrolysis— this leads to upregulating activation of the MAPKinase pathway (Xu et al. 2014).

Metastatic Disease and Dissemination to the Liver

At the time of diagnosis, roughly 5% of patients present with metastatic disease (Woll et al. 1999). There are two contributing hypotheses as to why the liver is the major site of metastasis: 1) the liver provides a microenvironment conducive for engraftment of circulating melanoma cells and 2) homing of tumor cells to the liver by secreted ligands (Bakalian et al. 2008).

The epithelial to mesenchymal transition of primary tumor cells promotes intravasation into the bloodstream and ensuing distant metastases. Although it is still unknown what factors specifically promote dissemination of uveal melanoma cells from the eye, research has implicated both ZEB1 and Twist1 as mediators of EMT (Asnaghi et al. 2015). TWIST1 and ZEB1 are known repressors of E-cadherin transcription, mediating loss of E-cadherin, which allows tumor cells to assume a more invasive and motile phenotype (Cantore et al. 1994). However, research by

Onken and associates, suggests a paradoxical role for E-cadherin in UM metastasis.

As previously mentioned, GEP class 2 uveal melanomas have a higher propensity to metastasize (Onken et al. 2004). Gene ontology revealed that class 2 tumors exhibited epithelial-like features by down-regulating neural crest and melanocyte-specific genes and up-regulating epithelial specific genes such as expression of E-cadherin (Onken et al. 2006). There are no lymphatics in the eye and therefore uveal melanoma cells exclusively metastasize hematogenously (Woll et al. 1999). Up-regulation of E-cadherin is associated with gastric cancers that hematogenously metastasize to the liver and advanced hepatocellular carcinoma. Similarly, cutaneous melanomas in advanced stages re-express E-cadherin. E-cadherin up regulation in class 2 melanomas may confer anchorage independent growth that allows tumor cells to dissociate from the primary tumor and survive during transit in the bloodstream to distant sites (Onken et al. 2006).

Hypoxia in the primary tumor promotes intravasation by inducing production of hypoxia factors and MMP's that increase vascular permeability (Lu and Kang 2010). Circulating tumor cells first encounter capillary beds in the lungs via pulmonary circulation, yet uveal melanoma predominantly metastasizes to the liver (Bakalian et al. 2008). One hypothesis for the mechanism behind this selective metastasis is Paget's "Seed and Soil" theory, postulating that the liver microenvironment provides a "fertile" niche for the tumor cells to survive and proliferate (Vidal-Vanaclocha 2008). Studies have shown high levels of c-Met expression in the primary tumor of patients who developed liver metastasis (**Figure**

2) (Bakalian et al. 2008). Research has shown that hepatocyte growth factor (HGF), the c-Met receptor ligand, is secreted by the liver into the blood stream; thereby, creating a gradient that contributes to liver specific metastasis (Mallikarjuna et al. 2007, Bakalian et al. 2008). In vitro experiments with primary uveal melanomas have shown that human uveal melanoma cells become highly motile and invasive in the presence of HGF, further supporting the suggested mechanism (Woodward et al. 2002). Recent work with uveal melanoma has also shown that some tumors express the chemokine receptor CXCR4 (**Figure 2**). CXCR4 activation by stromal derived factor-1 (SDF1) leads to a variety of signal transduction pathways, and regulation of cellular survival, proliferation, adhesion, and migration. It is hypothesized that uveal melanoma cells exploit this system to extravasate and home to the liver through the chemotactic gradient (Bakalian et al. 2008, Grossniklaus 2013).

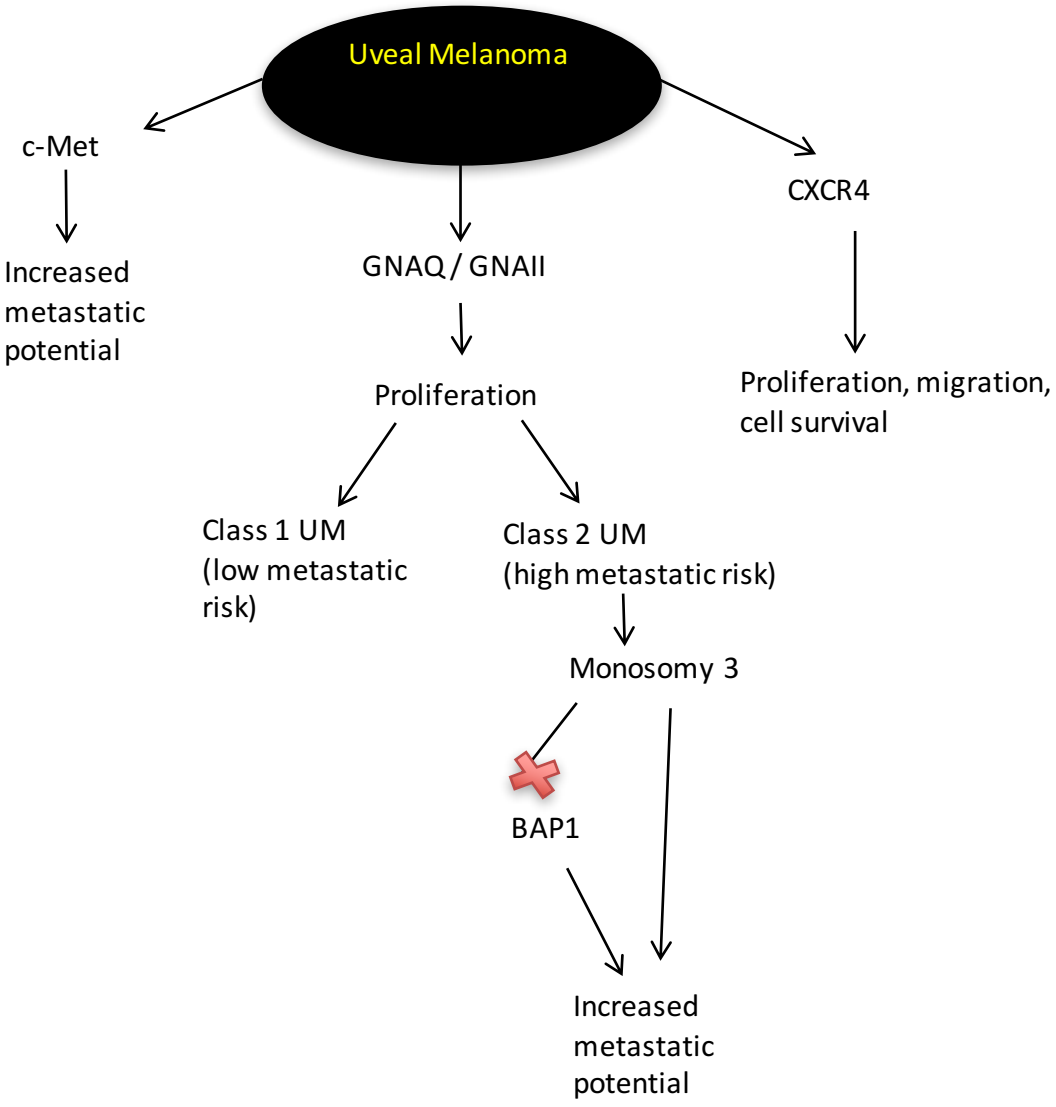

Figure 2. Pathways to tumorigenesis in uveal melanoma. Mutations in GNAQ/GNAII occur early in tumorigenesis and are hypothesized to be important in initial tumor development (Eagle 2013, Xu et al. 2014). Constitutive activation of GNAQ or GNA11 leads to upregulating activation of the MAPKinase pathway (Xu et al. 2014). Uveal melanoma primary tumors have been shown to express high levels of c-Met. The liver secretes HGF, the receptor ligand of c-Met, into the bloodstream and uveal melanoma cells exploit this chemotactic gradient to metastasize to the liver (Mallikarjuna et al. 2007, Bakalian et al. 2008). Some uveal melanoma tumors also express the chemokine receptor CXCR4. CXCR4 is activated by SDF1, and activation by SDF1 leads to multiple pathways regulating cellular survival, proliferation, adhesion, and migration GEP data revealed that class 2 melanomas have increased genomic instability and chromosomal abnormalities such as monosomy 3. Loss of chromosome 3 confers increased metastatic potential and is strongly correlated with somatic mutation of the gene BAP1 (Landreville et al. 2008, Harbour et al. 2010). BAP1 mutation leads to increased metastatic competence and has been implicated as a therapeutic target

Liver Microniche in Progression from Micrometastases to Macrometastases

The liver filters venous blood from the intra-abdominal viscera and about 30% of cardiac output which makes the organ a common site of metastasis for circulating tumor cells (Vidal-Vanaclocha 2008). The hepatic lobule is shaped like a hexagon **(Figure 3A)**. Six repeating patterns of blood vessels, or portal tracts, comprise the six corners of the lobule. The portal tract contains the portal venule, hepatic arteriole, and bile duct. At the center of the lobule is the central lobular vein, which drains deoxygenated blood from the sinusoids. The portal vein, including branches of the splenic vein, gives rise to portal venules and the hepatic artery gives rise to the hepatic arterioles. The portal venule and hepatic arteriole feed the sinusoidal space, which is lined by endothelial cells and resident macrophages, also known as Kupffer cells, and forms a microvasculature among the hepatocytes of hepatic lobule. Hepatocytes and fibroblasts, called hepatic stellate cells, surround the sinusoidal spaces. Blood from both the hepatic arteriole and portal venule flows through the sinusoidal space and drains into the central lobular vein where it is returned to systemic circulation (Vidal-Vanaclocha 2008). The liver's importance in circulation and filtration makes the organ a potential stopping point for circulating tumor cells. Metastatic tumor cells are filtered through the sinusoidal space and this filtration leads to mechanical arrest of tumor cells either in the periportal or lobular spaces **(Figure 3B)**(Vidal-Vanaclocha 2008, Grossniklaus 2013).

The liver presents a unique environment for tumor cells. There is evidence that once in the liver, uveal melanoma cells are able to form dormant micrometastases (Grossniklaus 2013). These dormant metastases are then able to

progress from dormant stage 1 metastases to avascular stage 2 metastases to vascularized stage 3 metastases following an "angiogenenic switch" (Grossniklaus 2013). Hepatic stellate cells and fibroblasts can respond to tumor-derived factors and contribute to blood vessel generation and tumor associated stroma (Vidal-Vanaclocha 2008). Activated hepatic stellate cells become smooth muscle actin-positive myofibrasts and invade the tumor area providing the metastatic cells with scaffolding for tumor growth prior to new blood vessel development (Vidal-Vanaclocha 2008, Grossniklaus 2013). Micrometastasis are also able to co-opt off the existing vasculature or serum in the sinusoidal space. Vascular endothelial growth factor (VEGF) stimulates endothelial cell growth and tumor angiogenesis. VEGF is overexpressed in uveal melanoma and is correlated with tumor growth (Yang et al. 2010). Tumor cells can also induce production of pro-inflammatory cytokines from tumor-activated endothelial cells that promote tumor-endothelial cell adhesion and VEGF-dependent proliferation (Vidal-Vanaclocha 2008, Grossniklaus 2013).

Nodular and Infiltrative Growth Patterns

There are two observed metastatic growth patterns of uveal melanoma in the liver. Tumors grow either adjacent to the portal venule effacing the surrounding hepatic parenchyma, or the tumors invade hepatic lobule and replace healthy hepatocytes (**Figure 3C**); these patterns respectively are referred to as the nodular, and infiltrative patterns (Grossniklaus 2013). In the nodular pattern, the hepatocytes are pushed aside destroying the preexisting liver architecture and the hepatocytes are separated from the tumor cells by a thin layer of reticulin fibers.

Conversely, metastatic cells in the infiltrative pattern, invade the liver parenchyma without disturbing the pre-existing liver structure at the interface (Van den Eynden et al. 2013). Previous observations have shown that these distinct growth patterns are not random and must be the result of interactions between tumor cells and the microenvironment (Van den Eynden et al. 2013). These patterns may also be due to the first occurrence of tumor cells in either the lobule or adjacent to the terminal branch of the portal vein. Both of these patterns may be seen in the same liver (Grossniklaus 2013).

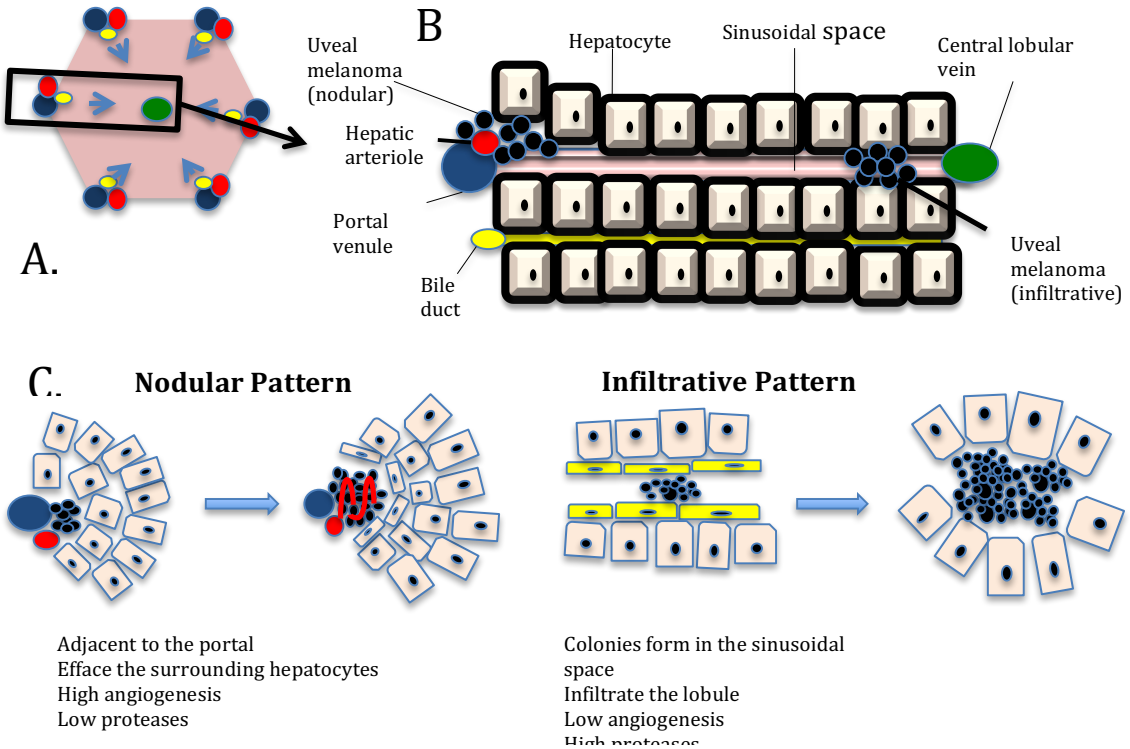

Figure 3 **Nodular Vs. Infiltrative Pattern. A)** The hepatic lobule is shaped like a hexagon with the portal triad repeating to form its 6 apices. The portal triad is comprised of a portal venule (blue), a hepatic arteriole (red), and a bile duct (yellow). Blood flows from the triad through the sinusoids to the central lobular vein (green). **B)** The sinusoidal spaces are lined by hepatocytes (tan) and endothelial cells (not pictured). Uveal melanoma cells metastasize hematogenously and arrive in the liver through the hepatic arteriole or portal venule. These circulating tumor cells can arrest in the hepatic lobule adjacent to the portal triad or within the sinusoidal space. **C)** In the liver there are two observed growth patterns of uveal melanoma. The nodular pattern in which melanoma cells are adjacent to the portal venule, and efface the surrounding hepatocytes. In the infiltrative pattern, tumor cells fill the sinusoidal space, kill, and replace healthy hepatocytes (Grossniklaus et al. 2014).

Intrinsic Defense of the Hepatic Sinusoid

In the liver, cytotoxic and phagocytic immune cells preferentially reside in the sinusoids and periportal area of the hepatic lobule. In the sinusoids these cells are able to remove most circulating tumor cells, derived primary metastases, that pass through the liver (Vidal-Vanaclocha 2008). Kupffer cells, NK cells, and endothelial cells coordinate the major defense mechanisms of the liver against circulating tumor cells (Vidal-Vanaclocha 2008). Hepatic sinusoidal endothelial cells (HSECs) line the sinusoids of the hepatic lobule. Clusters of invading tumor cells can block sinusoidal spaces, inducing ischemia and subsequent inflammatory response (Van den Eynden et al. 2013). In response, local HSECs and Kupffer cells release nitric oxide and reactive oxygen species, which can lead to tumor cell damage and death. Kupffer cells are tumoricidal bone-marrow derived macrophages than can phagocytose and clear cancer cells (Vidal-Vanaclocha 2008, Van den Eynden et al. 2013). Kupffer cells can also release cytokines, like IFN-γ, that modulate the innate immune response by activating other immune cells such as hepatic NK cells (Vidal-Vanaclocha 2008, Van den Eynden et al. 2013).

Role of the Immune Response and Natural Killer Cells in Tumor Progression

The immune response to cancer is well known to have both an inhibitory effect and tumor-promoting effect on regulation of metastasis. Natural killer cells (NK cells) are large granular lymphocytes that are a part of the innate immune response, and have cytolytic activity against tumor cells and infected cells (Harning et al. 1989). The “missing self” hypothesis states that NK cells are able to recognize and eliminate cells that do not express major histocompatibility complex (MHC)

class I molecules. NK cells have the ability to differentiate between normal and aberrant cells, and in turn lyse cells that are transformed, or virus infected (Hans-Gustaf 1990). The MHC molecule binds peptides from pathogens and presents them on the cell surface for T-cell recognition. NK cells can kill certain tumors with low or no expression of MHC 1 class molecules; however, studies have shown that it is difficult to identify what modifications in MHC expression cause NK cells to either lyse or spare abnormal cells (Hans-Gustaf 1990).

There is increasing evidence that NK cells eliminate metastatic uveal melanoma cells in the liver (Yang et al. 2004). Expression of MHC is necessary for an effective anti-tumor T-cell response; however, the presence of MHC class I molecules suppresses NK cells (Blom et al. 1997). NK cells are able to eliminate tumor cells expressing low MHC class I in the liver (Yang et al. 2004). In uveal melanoma patients, high expression of MHC was correlated with death from metastases, suggesting that NK cells play an essential role in immune response to uveal melanoma metastases (Blom et al. 1997). NK cell depletion leads to significant reduction in the clearance of uveal melanoma cells from the liver and more extensive metastases (Ma et al. 1995). Previous experiments in the Grossniklaus lab showed that enhanced hepatic NK cell activity induced by IFN- α2b treatment decreased hepatic micrometastases (Yang et al. 2004). The proposed mechanism for NK cell anti-tumor activity is through a series of autocrine and paracrine loops **(Figure 4)**. Following endothelial cell damage in the sinusoidal space, caused by micrometastases, the damaged endothelial cells secrete IL-12 and express vascular adhesion molecule (VCAM) -1, -4, -6, which recruit NK cells to the sinusoidal space.

NK cells secrete IFN-γ, a cytokine that is essential to innate and adaptive immunity, which potentiates macrophage and NK activity. IFN- α2b enhances NK cell activity by boosting IFN-γ expression by NK cells (Yang et al. 2004). IFN-γ secretion also further potentiates NK cell activity by stimulating T-lymphocytes that secrete IL-10. Secretion of IL-18 and IL-12 by the damaged endothelial cells, directly recruits B-lymphocytes, which also potentiate NK cell activity (Yang et al. 2004). While NK cells have a cytolytic effect on uveal melanoma cells, they also block basic fibroblast growth factor (bFGF) and tumor angiogenesis (Harning et al. 1989, Yang et al. 2004).

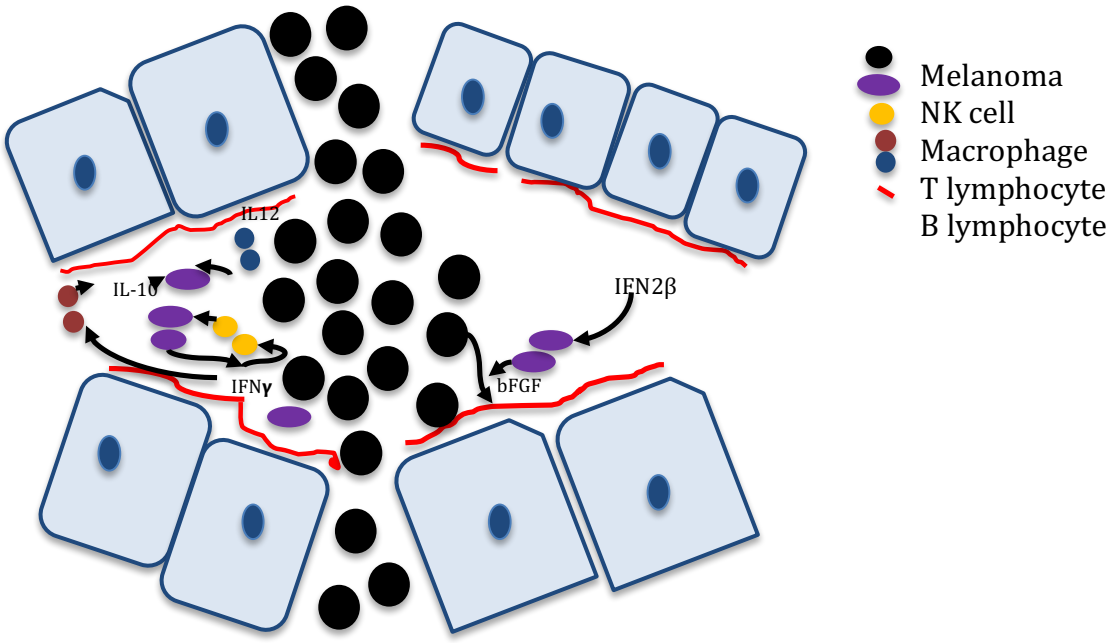

Figure 4 **Proposed Mechanism of Interferon enhanced NK cell activity.** Hepatic micrometastases in the sinusoidal space cause sinusoidal endothelial cell damage. In response, damaged endothelial cells secrete IL-12 and express VCAMs -1, -4, -6, which recruit NK cells to the sinusoidal space. IFN- α2b enhances the activity of IFN- γ expressing NK cells. IFN- γ produced by the NK cells also stimulates T-lymphocytes to secrete IL-10, which further potentiates NK cell activity. Secretion of IL-12 by damaged endothelial cells also recruits B-lymphocytes to the sinusoidal space. The B-lymphocytes further potentiate NK cell activity. In addition to the direct melanoma-killing effect, NK cells block bFGF thus downregulating angiogenesis (Yang et al. 2004).

Anti-Asialo GM1 induced NK deficiency

Anti-asialo GM1 is a rabbit polyclonal antibody that reacts with asialo ganglio-N-tetraosylceramide (asialo-GM1), a glycoprotein that is present on mouse NK cells and a subset of monocytes. The antibody specifically recognizes asialo-gm1 and not other glycolipids (eBioscience). A detailed mechanism of the in vivo effects of anti-asialo GM1 remains unclear, but the decrease in NK cells is attributed to ab-mediated lysis. NK cell activity is effectively abolished with repeated injection of anti-asialo GM1 serum (Habu et al.). In a study conducted by the Grossniklaus lab, NK cell depletion by cytotoxic treatment with anti-asialo GM1 resulted in greater hepatic tumor burden (Dithmar et al. 1999). The study used B16LS9 murine melanoma cells, which also express low levels of MHC class I and high levels of c-MET, similar to human uveal melanoma. Human uveal melanoma cells that express low levels of MHC class I molecules are susceptible to NK cell-mediated lysis in vitro and in vivo (Dithmar et al.).

VEGF: PEDF Ratio Mediates Tumor Progression

Vascular endothelial growth factor (VEGF) and pigment epithelium-derived factor (PEDF) both play a central role in tumor angiogenesis and stromagenesis (Lattier et al. 2013). Angiogenesis is essential for tumor progression from micro- to macro-metastases (Hicklin and Ellis 2005). As tumor cells become hypoxic they secrete VEGF, thus recruiting host vascular endothelial cells to the metastatic area (Lattier et al. 2013). Stromagenesis provides a scaffold for new blood vessels and tumor growth, by activating hepatic stellate cells into a migratory state and also forming ECM components such as type I and type II collagen (Vidal-Vanaclocha

2008, Lattier et al. 2013) PEDF, produced by hepatocytes, inhibits angiogenesis and stromagenesis (Dawson et al. 1999, Lattier et al. 2013). PEDF inhibits angiogenesis by inducing endothelial cell apoptosis through various apoptotic pathways including Fas/FasL and cleavage of caspases 8 and 9 (Volpert et al. 2002, Chen et al. 2006, Lattier et al. 2013). PEDF exerts its anti-angiogenic effect on VEGF by inhibiting ligand binding to VEGF receptors 1 and 2 (Cai et al. 2006, Zhang et al. 2006). PEDF also induces apoptosis in HSC's, inhibiting stromagenesis (Ho et al. 2010, Lattier et al. 2013). Hypoxia induces degradation of PEDF by matrix metalloproteinases MMP-2 and MMP-9, which are secreted by tumor cells (Notari et al. 2010, Lattier et al. 2013). This finding suggests that in a hypoxic environment, tumor cells are able to down-regulate host PEDF as they progress (Fernandez-Barral et al. 2012, Lattier et al. 2013). The VEGF:PEDF ratio is increased as tumor cell production of VEGF continues uninhibited by PEDF which is normally produced by host hepatocytes. An increase in the VEGF:PEDF ratio is a proposed mechanism for "angiogenic switch" in uveal melanoma (Yang et al. 2006). In a study done by Lattier et al., knockout of host PEDF led to increased metastatic progression. When host PEDF is lost, there was increased prevalence of macrometastases (< 200 um), and mean vascular density increased in metastatic tissue. These findings suggest that when the VEGF: PEDF ratio is increased stromagenesis and angiogenesis are potentiated in metastatic tissue resulting in tumor progression. Host PEDF has a clear effect on preventing tumor progression (Lattier et al. 2013). In addition to hepatocytes, fibroblasts, or hepatic stellate cells, are able to produce PEDF that attenuates progression of metastatic melanoma. Recent research has shown that melanoma cells are able to

induce the tumor-promoting phenotype of cancer-associated fibroblasts by inhibiting the tumor-suppressive properties of fibroblasts. Melanoma cells secrete PDGF-BB and TGF-β, which suppresses fibroblast-derived PEDF in tumor-associated fibroblasts (Nwani et al. 2016).

Central Hypothesis and Project Focus

The purpose of my work is to determine if PEDF and NK cells are able to attenuate the progression of metastatic uveal melanoma in the nodular and infiltrative pattern. There are two hepatic compartments involved in the metastatic process: the periportal area, and sinusoidal spaces. In the nodular pattern of metastasis, tumors become established adjacent to the portal venule and efface the surrounding hepatocytes; whereas, in the infiltrative pattern of metastasis tumors invade the sinusoidal space and replace the hepatic lobule. Preliminary data shows that PEDF and NK cells have important protective roles against the progression of micro- to macro-metastases. Our reasoning is host PEDF, produced by hepatocytes and stromal cells, prevents growth of metastases in the nodular pattern based on previous observations that show when host PEDF is knocked out melanoma cells in the nodular pattern are able to proliferate in the periportal area by co-opting the vasculature of the portal triad. Preliminary observations have shown that NK cells are recruited to the sinusoidal spaces, and elimination of NK cells allows melanoma cells to evade being targeted by the innate immune response, thus enabling the tumor cells to proliferate in the sinusoidal space by receiving nourishment from serum that is present. In order to further investigate these observations, we hypothesized that the uveal melanoma mouse models, where NK cell infiltration or

PEDF secretion would be interrupted would exhibit different ratios of the infiltrative and nodular growth patterns versus controls. The nodular pattern would predominate in the PEDF KO model due to loss of PEDF's antagonistic effect on tumor cell-mediated angiogenesis in the periportal area. NK cell deficient mice would predominantly exhibit metastases of the infiltrative pattern due to the absence of NK cell protection in the sinusoidal space. Lastly, to address this hypothesis, we designed three mouse melanoma models by injecting B16LS9 melanoma cells into the right eye of mice with C57BL6 background. The cells were allowed to metastasize to liver, and the liver was histologically evaluated for metastasis type, size, and distribution. Tumor vascularization was also examined through quantification of mean vascular density. FACS analysis was utilized to measure NK cell activity and to investigate the effect of NK cell depletion on other hepatic lymphocyte populations.

Methods and Materials

Cell Culture

Mouse melanoma cell lines B16-LS9 were cultured at 37°C in a 5% CO2 incubator. The complete culture medium included RPMI1640 with HEPES, L-glutamine, 10% FBS, 1% nonessential amino acids, 1% sodium pyruvate solution, 1% MEM vitamin solution, and a 1% antibiotic-antimycotic solution. Cells were grown to 90% confluence, and then they were washed three times with Hank's solution, trypsinized and expanded for use in all experiments (Yang et al. 2004).

Mouse Model

Eight-week old mice were obtained from a Jackson Laboratories (Bar Harbour, ME). All experiments were performed in compliance with the Association for Research in Vision and Ophthalmology (ARVO) Statement for the use of animals in Ophthalmic and Visual Research and with the Institutional Animal Care and Use Committee policies and procedures. B16-LS9 mouse melanoma cells (courtesy of Dario Rusciano, Friedrich Miescher Institute, Basel Switzerland) were chosen because they mimic human disease progression of melanoma cell metastasis to the liver, express high levels of c-Met, and fail to express MHC class I antigen as demonstrated in previous experiments (Diaz et al. 1999, Dithmar et al. 1999). All mice used in this experiment were C57BL/6 background and injected with B16LS9 murine melanoma cells to ensure that genetic variability and immune competence did not affect the results apart from the manipulated variable.

Inoculation of Melanoma Cells into the Posterior Compartment of the Eye

Eight-week old female C57BL/6 mice and C57BL/6 PEDF KO mice with healthy eyes were inoculated in the uveal layer of the right eye with $5x\ 10^5$ B16-LS9 melanoma cells in 2.5µL phosphate buffer solution. The mice were anesthetized by intraperitoneal injection of 100mg/kg ketamine and 12mg/kg xylazine mixture in phosphate buffer solution. The cells were injected into the posterior compartment of the right eye by preparing a passageway with a 30-gauge needle under guidance of a dissection microscope. The inoculated eyes were enucleated after one week and 28 days post injection the mice were euthanized and livers were collected and routinely processed for histological evaluation (Diaz et al. 1999, Yang et al. 2004, Lattier et al. 2013).

Anti-Asialo Gm1-mediated NK Cell Depletion

One group of 15 female C57BL/6 mice was treated with anti-asialo gm1 serum to deplete NK cells. Anti-Asialo GM1 (Rabbit; Wako Pure Chemical Industries, Osaka, Japan) stock solution was prepared with 1mL of sterile water. Anti-asialo Gm1 stock was diluted (1:4) before injection with 1mL of stock solution and 3 mL of phosphate buffered solution. Mice were given 100 uL IP injections of the anti-asialo Gm 1 serum every 3 days beginning two weeks before inoculation continuing until they were euthanized (Yang et al. 2004)

Metastasis, Frequency, and Stage Assays

The livers were grossly examined, and submerged in 4% neutral buffered formaldehyde for routine processing. Formalin fixed-paraffin embedded slides were

stained with hematoxylin and eosin (H&E) and microscopically evaluated (Olympus) for metastases. Three sections through the center of each liver were evaluated for the number of metastases, and the average number per section was determined, as previously described (Diaz et al. 1999, Yang et al. 2004). To determine relative metastasis area the sizes of all metastases in a single liver section were added to calculate a total metastasis area (μm^2) and averaging this value per mouse. Metastases were also separated by size into stage 1 micrometastases (<50 μm in diameter), stage 2 intermediate metastases (50-200 μm), and stage 3 macrometastases (>200 μm). These measurements were also performed in triplicate sections and averaged per mouse (Lattier et al. 2013).

Evaluation of tumor vascular density

The number of blood vessels per area for metastatic tissue was determined through H&E staining. The number of blood vessels per 40x high-powered field (HPF) was calculated and averaged to mean vascular density. An individual vessel was defined as an area of lumen lined with endothelial cells, while tracts and branches were counted as separate vessels (Lattier et al. 2013).

Liver Processing for FACS

Mouse livers were processed 24 hours after isolation. Livers were placed in small dishes with 5mL of RPMI media. Tissue was macerated using a Cell Strainer Pestle (MIDSCI). The resultant cell suspension was filtered using a Falcon 70um nylon strainer (BD Biosciences, San Jose, CA) followed by centrifugation at 1500 RPM x 7

minutes at RT. Cells were resuspended in PBS/1% FBS (Lonza, Walkersville, MD) and kept on ice until ready for use (Morales, unpublished).

Cell surface labeling

Cell viability was evaluated at the time of cell dissociation. The following primary antibodies were used to detect surface antigens by incubating the cells on ice for 30 minutes: anti-CD3 (clone 17A2), Brilliant Violet 605, anti-CD4 (clone GK1.5) PerCP-Cy5.5, anti-CD8a (clone 53-6.7) PE-Cy7, anti-NK1.1 (clone PK136) APC, anti-CD49b (clone DX5) PE, anti-CD45R/B220 (RA3-6B2) PE-Cy7, anti-CD19 (clone 6D5) PerCP-Cy5.5, anti-CD11b (clone M1-70) PE, anti-CD11c (clone N418) Brilliant Violet 421, and anti-Ly-6G/Ly-6C (GR-1) [clone RB6-8C5] APC. All anti-mouse antibodies were purchased from BioLegend. Samples were washed 3x with PBS/1% FBS. Data acquisition was done in BD Biosciences LSRII Flow Cytometer and data analysis performed using FlowJo vX.0.0.6 (Morales, unpublished).

Statistical Analysis

To compare the three groups (PEDF KO, NK cell deficient, and WT C57BL6) a one-way ANOVA with Tukey's post-test was performed for all assays to determine statistical significance among groups. When comparing metastasis type among the three groups a two way ANOVA and Tukey's post-test was utilized to determine statistical significance. The value $p<0.05$ was used to define statistical significance for all assays. All data was reported with standard error of the mean.

Results

[A]. Effects of NK cell depletion and PEDF KO on metastasis frequency and size

Three sections through the centers of each liver were microscopically examined for metastases, and the average number of metastases per liver section was determined. There was no statistically significant difference in the number of metastases per section between the wild-type and PEDF KO genotype. Natural killer cell deficient mice showed a statistically significant increase in the number of metastases per liver section with a 2.8-fold increase over the wild-type (**Figure 5**). These data show that NK cell depletion increases the number of hepatic metastasis.

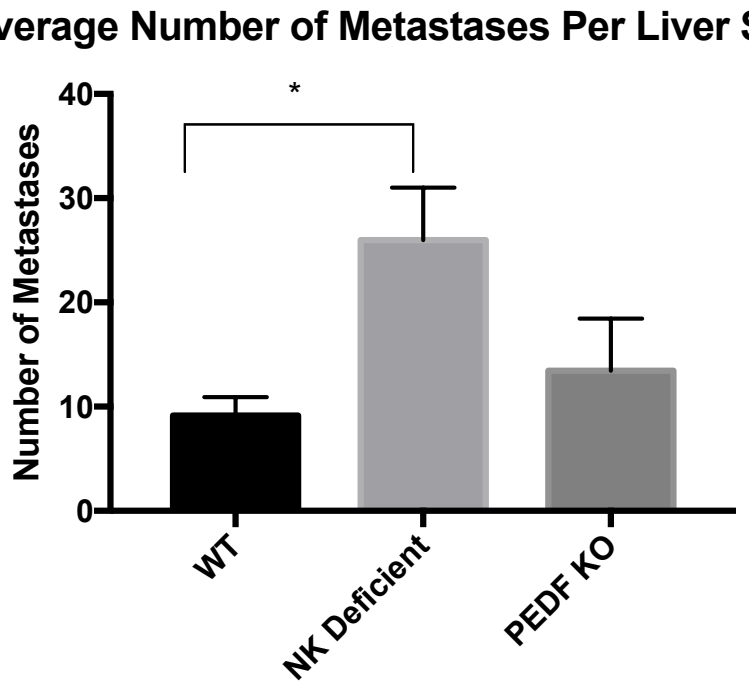

Figure 5. Loss of NK cell increases the number of hepatic metastases per liver section. The total number of metastases per liver section without respect to size was counted to determine the average. NK cell deficient mice showed a 2.8-fold increase in hepatic metastases over wild-type mice. Data are reported with standard error of the mean, n=9, n=9, n=8 respectively, *p<.05 using one-way ANOVA with Tukey's post-test.

Wild-type mice livers predominantly had hepatic stage 1 metastases while NK cell deficient and PEDF KO mice had increased numbers of stage 2 and stage 3 metastases (**Figure 6A**). NK cell deficient mice had a statistically significant increase in stage 2 metastases over the wild-type and PEDF KO genotypes. Wild-type mice showed no stage 3 metastases while PEDF KO and NK cell deficient mice contained a greater number of stage 3 metastases. NK cell deficient mice had tumors that were grossly visible upon initial examination (**Figure 6B**). These data demonstrate that loss of PEDF and NK cell function leads to a significant increase in the size of hepatic metastases.

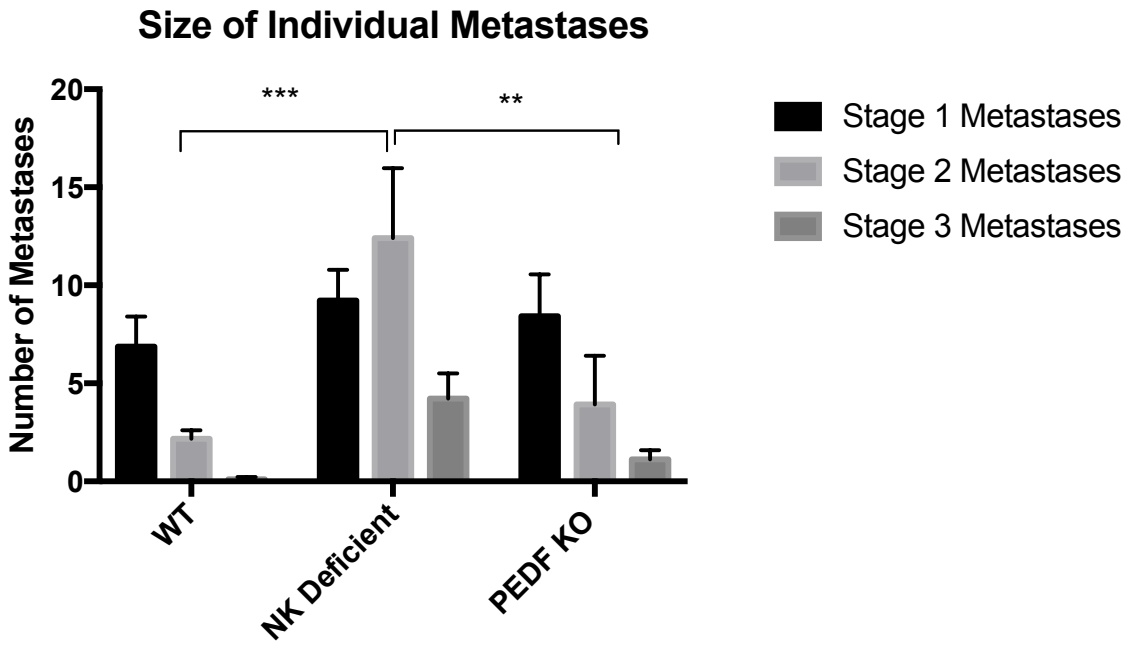

Figure 6A. NK cell deficient mice showed statistically significant increase in the number of stage 2 metastases. The size of individual metastases was measured in each of the 3 mouse models and staging was determined as stage 1 (<50 μm), stage 2 (50-200 μm), and stage 3 (>200 μm). Wild-type mice livers contained no stage 3 metastases, while NK cell deficient and PEDF KO had an increased number of stage 2 and stage 3 metastases. NK cell deficient mice had a 5.7-fold increase in stage 2 metastases over wild-type mice, and 3.2-fold increase over PEDF KO mice. Data are reported with SEM, n=9, n=9, and n=8 respectively, **p<.01, ***p<.001, using two-way ANOVA with Tukey's post-test.

Figure 6B. Grossly visible macrometastases from NK cell deficient mice. Macrometastases that were visible to the naked eye following liver harvesting from NK cell deficient mice. These metastases disrupt normal liver function and usually lead to liver failure and death.

[B]. Effects of NK cell depletion and PEDF KO on ratio of infiltrative: nodular pattern

Depletion of NK cells had no effect on the ratio of infiltrative: nodular pattern of hepatic metastases. However, PEDF KO mice had an increased percentage of nodular metastases, which was statistically significant increase in comparison to wild-type (**Figure 7**). These data show that PEDF has an inhibitory effect on the nodular pattern of growth. NK cell deficient mice had a statistically significant increase in the number of stage 2 nodular metastases in comparison to wild-type mice, and an increase in stage 2 infiltrative in comparison to both wild-type mice and PEDF KO mice. There was no statistical significance in the number of stage of 3 hepatic metastases (**Figure 8, Figure 9**). However, PEDF KO mice had a greater number of stage and stage 3 nodular metastases, while NK cell deficient mice also had a greater number of stage 2 and stage 3 metastases of both nodular and infiltrative pattern in comparison to wild-type mice. Wild-type mice showed no stage 3 metastases of either infiltrative or nodular pattern.

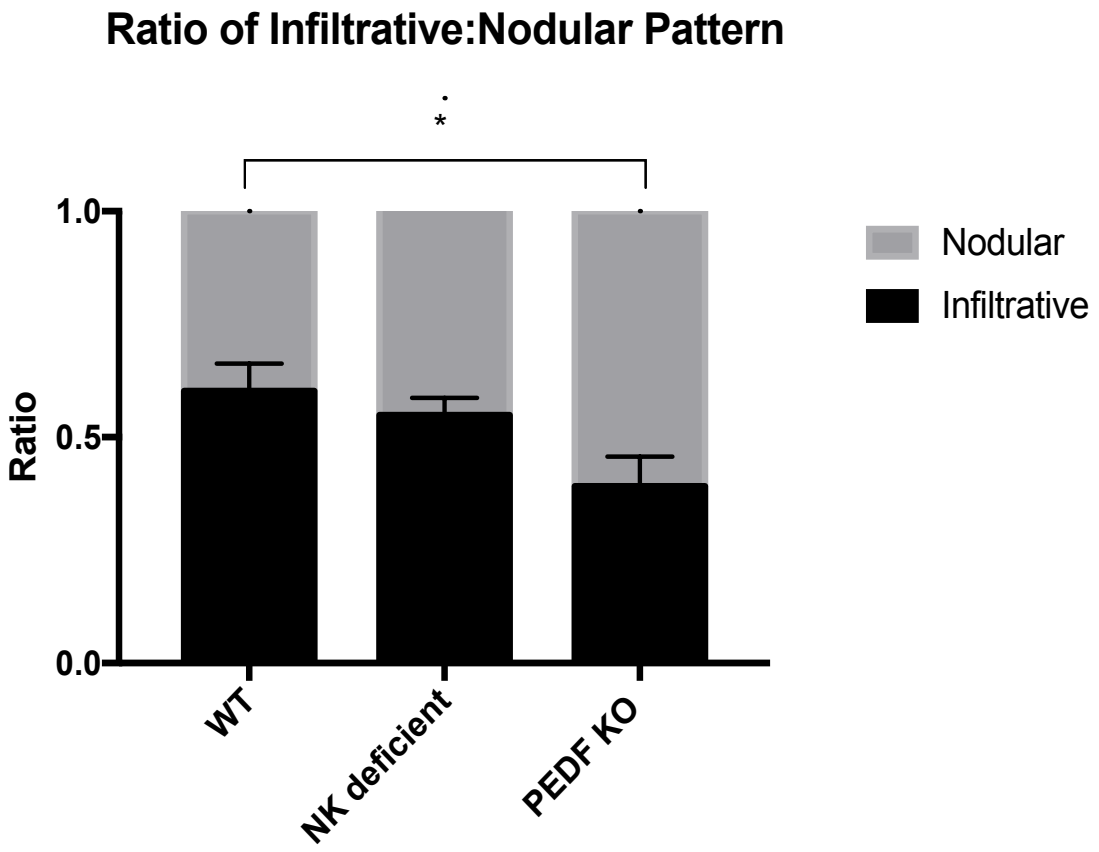

Figure 7. PEDF KO mice showed a greater nodular: infiltrative ratio than wild-type mice. The ratio of infiltrative to nodular metastasis was determined from the average number of infiltrative and nodular metastases per mouse. The ratios were then averaged for each group (wild-type, PEDF KO, and NK cell deficient) to establish an overall average for each experimental group. PEDF KO and NK cell deficient mice were compared to wild-type mice using a two-way ANOVA with Tukey's post-test. Data are reported with standard error of mean, n=9, n=9, n=8 respectively, *p<.05.

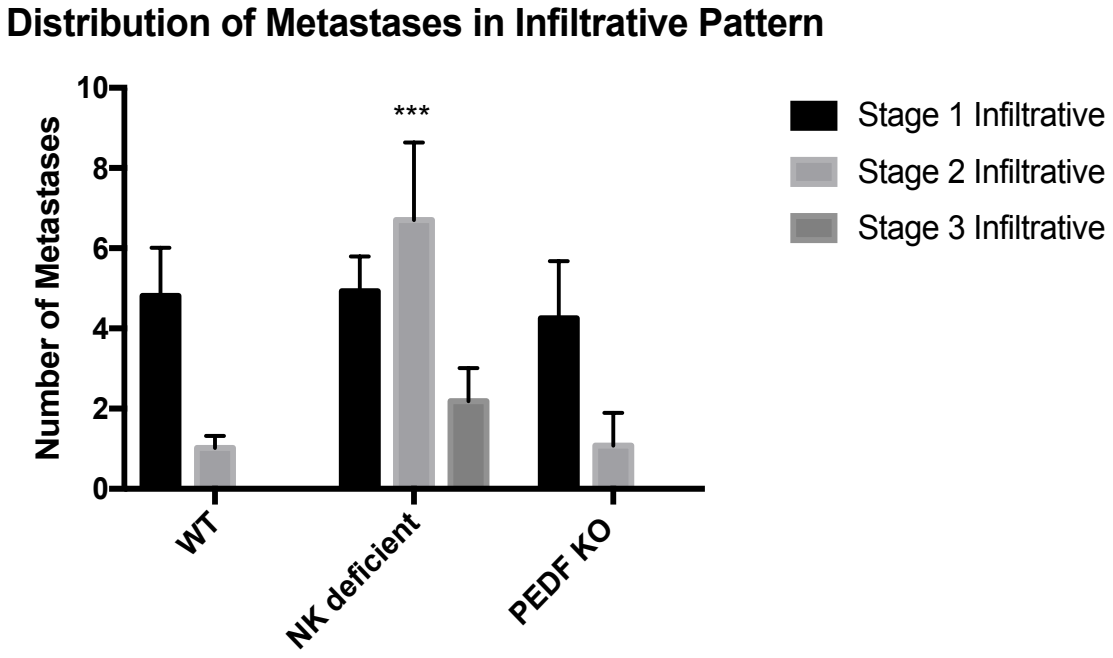

Figure 8. NK cell deficient mice showed statistically significant increase in the number of stage 2 infiltrative hepatic metastases. NK cell deficient mice had significant increase in the number of stage 2 infiltrative metastases in comparison to wild-type and PEDF KO mice. Data are reported with standard error of the mean, n=9, n=9, n=8 respectively, ***p<.001 using two-way ANOVA with Tukey's post-test.

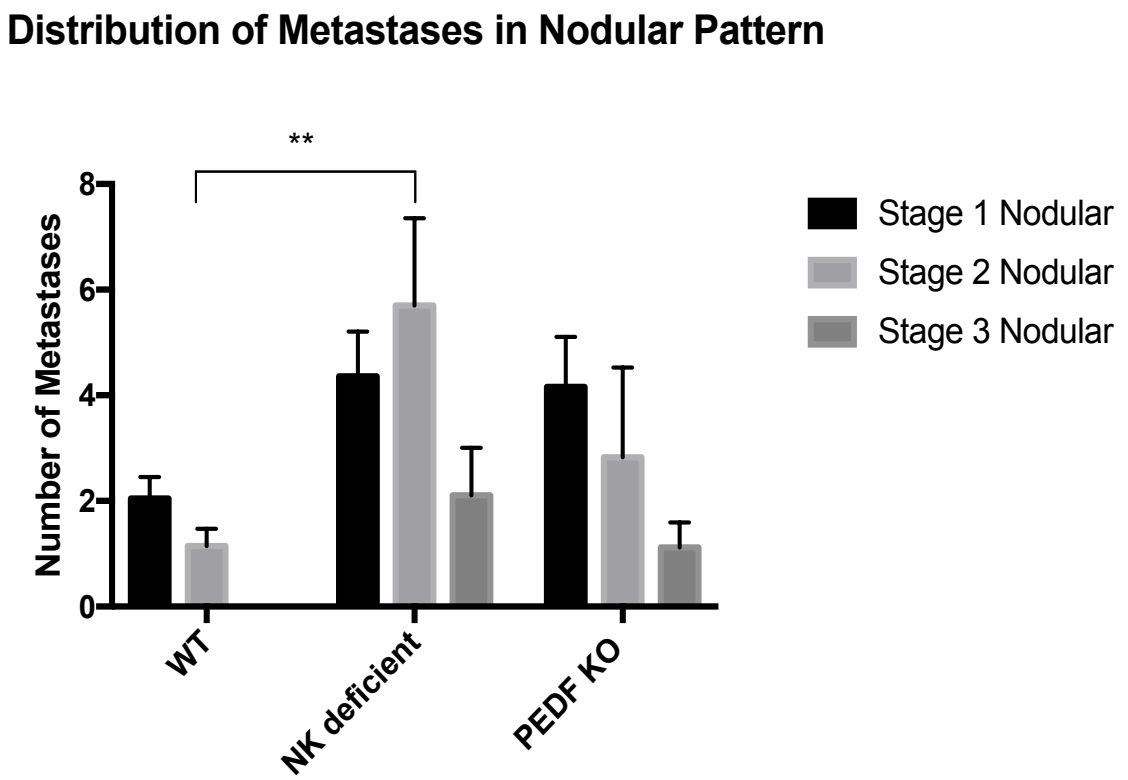

Figure 9. NK cell deficient mice showed statistically significant increase in the number of stage 2 nodular hepatic metastases. NK cell deficient mice had a significant increase in the number of stage two nodular in comparison to wild-type mice. There was no statistical significance in the number of stage of 3 metastases. However, PEDF KO mice had a greater number of stage 2 and stage 3 nodular metastases while wild-type mice predominantly showed stage 1 metastases. Data are reported as standard error of the mean, **p<.01, n=9, n=9, n=8 respectively, using two-way ANOVA with Tukey's post-test.

[C]. Effect of NK cell depletion and PEDF KO in mean vascular density of metastases.

As per previous results, PEDF KO mice showed the greatest increase in mean vascular density of metastatic tissue, or the number of blood vessels per 40x high power field of magnification (40HPF). NK cell depletion, did not have a direct impact on tumor angiogenesis. NK cell deficient mice had a slight increase in mean vascular density of metastatic tissue, but this difference was not statistically significant. This increase in MVD may be attributed to the increase in stage 3 metastases in NK cell deficient mice. PEDF KO mice showed a 9.1-fold increase in mean vascular density in comparison to wild-type mice, and a 3.2 increase in comparison to NK cell deficient mice (**Figure 10**). These results suggest that PEDF normally functions to inhibit angiogenesis in hepatic metastases.

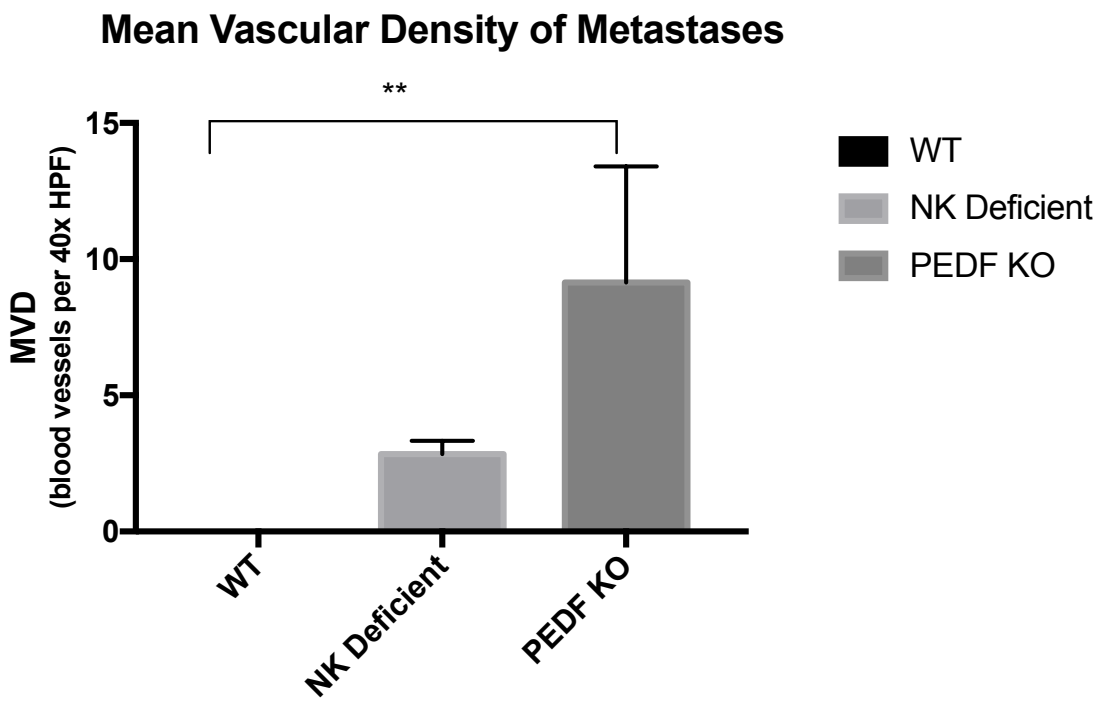

Figure 10. PEDF KO mice had statistically significant increased mean vascular density in metastatic tissue in comparison to wild-type mice. PEDF KO mice had 9.1-fold increase in mean vascular density in comparison to wild-type mice which showed no vascularization of metastatic tissue. Data are reported with standard error of the mean, **p <.01, n=9, n=9, n=8 respectively, using a one-way ANOVA with Tukey's post-test.

[D.] FACS analysis of NK cell population in mouse models

To induce NK cell deficiency, mice were injected intraperitoneally with anti-asialo GM1 antibody every 3 days beginning two weeks before inoculation and continuing until the mice were euthanized. Livers were collected and processed for FACS analysis to asses NK cell activity following treatment with anti-asialo GM1. FACS analysis revealed significant decrease in NK cells in the liver after 4 weeks of treatment with anti-asialo GM1(**Figure 11A**). These results indicate that anti-asialo GM1 treatment successfully caused NK cell deficiency in the treated group (**Figure 11B**).

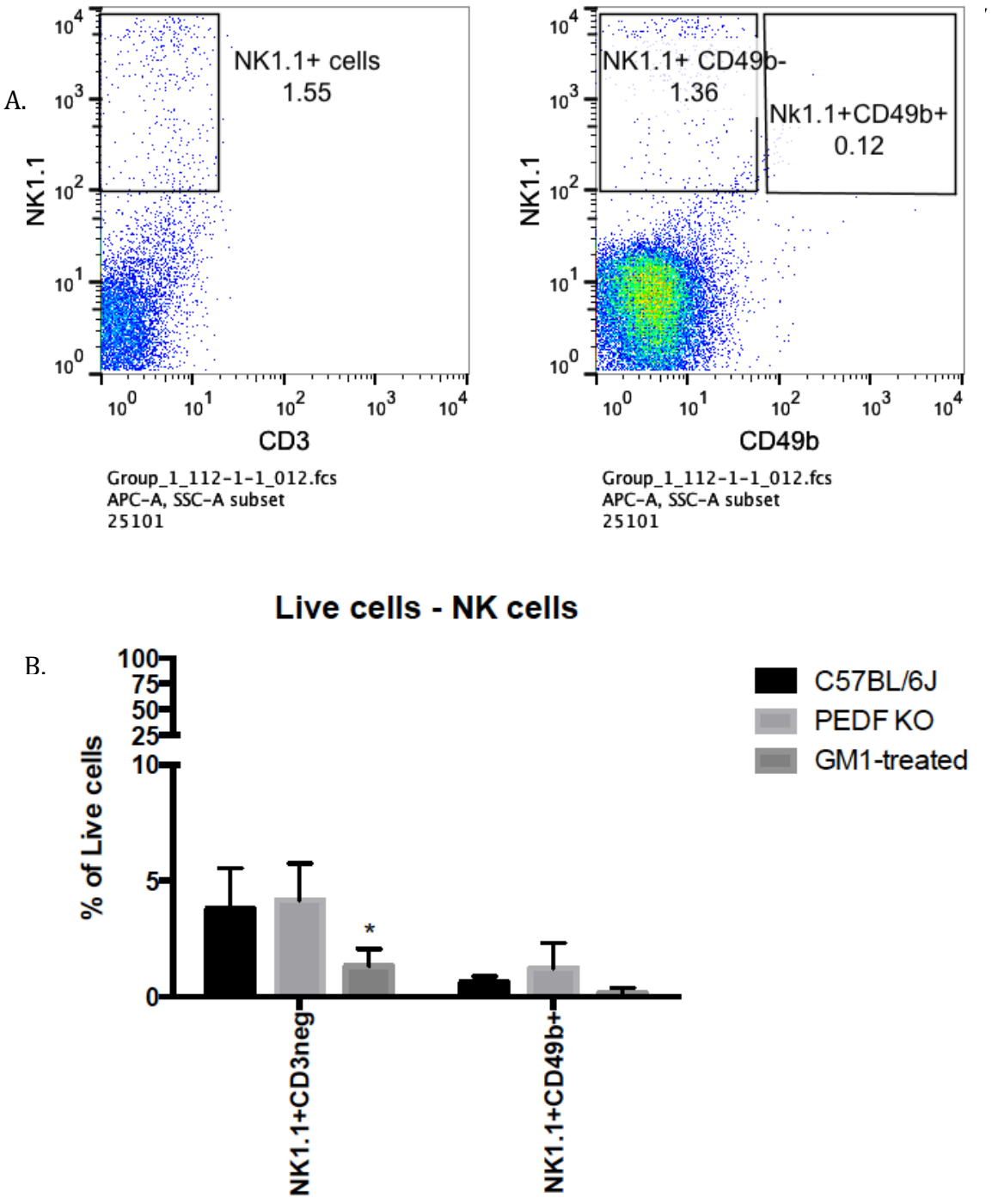

Figure 11. FACS analysis showed a statistically significant decrease in NK cells in the livers of GM1 treated mice. A. The number of NK cells as a percentage of live cells is shown. Livers were harvested from euthanized mice after 4 weeks of treatment with anti-asialo GM1. Livers were also collected from control and PEDF KO mice. The total cell population was stained with a cocktail of antibodies against CD3, Cd49b, and NK1.1 in order to quantify NK cells by FACS. NK 1.1 CD3- is a marker for all NK cells. CD49b is an integrin expressed by most NK cells. Cells expressing NK1.1 were further subdivided by the CD49b marker expressed by NKT cells. **B.** Anti-asialo GM1 injections significantly reduced NK cells in the livers of treated mice. Data are reported with standard error of the mean, *p<.05, n=3, using multiple t-tests (Morales, unpublished).

[E.] FACS analysis of T cells

FACS analysis of live T cells was also conducted to confirm that anti-asialo GM1 did not have cytotoxic effects on other lymphocyte populations in the liver. CD3+ is a marker for all T-cells. CD3+ CD4+ cells are helper T-cells. Most T cells in the liver are CD8+ T cells. CD8+ T cells have tumoricidal activity. There was no significant difference in T cell populations in the liver between wild-type mice, PEDF KO mice, and GM1 treated mice (**Figure 12**).

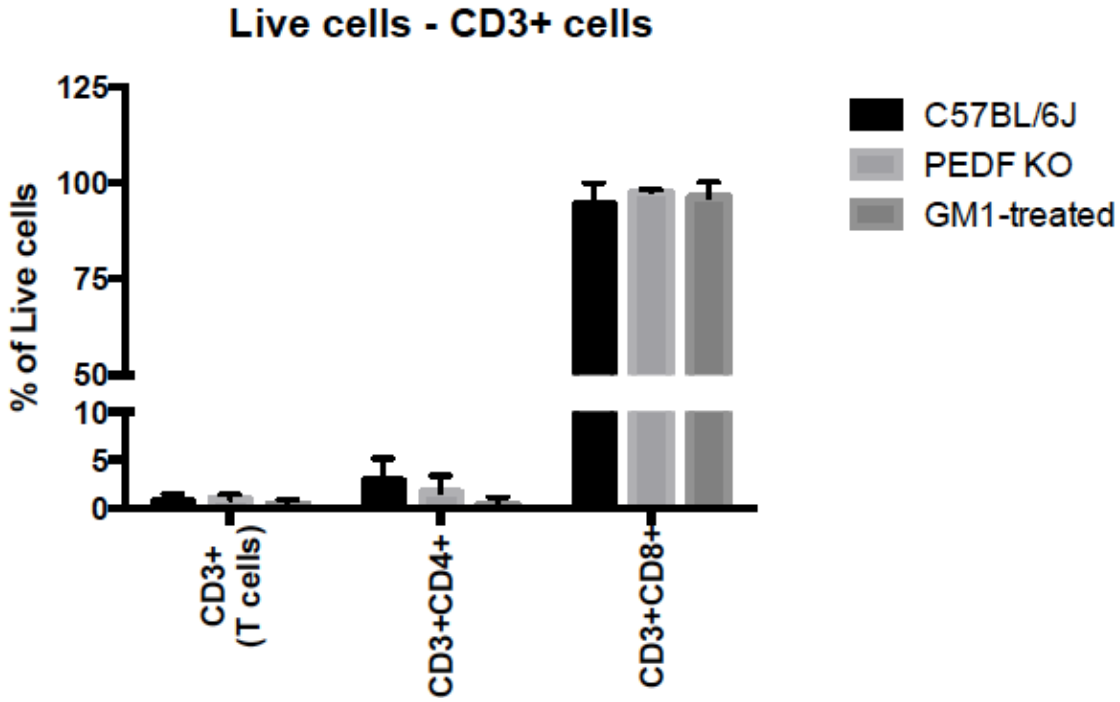

Figure 12. FACS analysis revealed that GM1 did not have a cytotoxic effect on CD8+ T cells in the livers of treated mice. CD3+ denotes lymphocytes with T-cell lineage. CD3+CD4+ lymphocytes classify a subset of regulatory T cells. Most T cells found in the liver are CD3+CD8+ cytotoxic T cells with anti-tumoricidal activity. There was no statistically significant difference in the percentage T cells in the livers of wild-type mice, PEDF KO mice, and GM1 treated mice. These data show that anti-asialo GM1 did not have a cytotoxic effect on T cell populations. Data are reported with standard error of the mean, *p<.05, n=3, using multiple t-tests (Morales, unpublished).

[F.] FACS analysis of B cell populations in mouse models

To determine the status of B cell populations in the liver, FACS analysis was used to quantify the percentage of mature B cells (B220+CD19+) with respect to all B cells (B220). Both PEDF KO and GM1 treated mice showed significant reduction in the CD19 expressing mature B cells (**Figure 13**). These results correlated with increased tumor progression in PEDF KO and GM1 treated mice suggesting that increased tumor burden may be affecting B cell maturation or vice versa. Further investigation of CD19 negative cells showed that there was significant reduction in the number mature dendritic cells expressing CD11c (CD19- CD11c+). CD11c negative cells are referred to as pre-plasmacytoid dendritic cells (McKenna et al. 2005). There was also significant reduction in CD11c+ CD11b+ myeloid dendritic cells (**Figure 14**). These results prompted further investigation into expression of myeloid derived suppressor cells (MDSCs) which are immature myeloid cells that potently suppress the immune response. MDSCs are Ly6G/C+ CD11b+ expressing cells. FACS analysis revealed a slight increase in the percentage of MSDC's expressed in PEDF KO, and GM1 treated mice however these results were not statistically significant (**Figure 15**).

A.

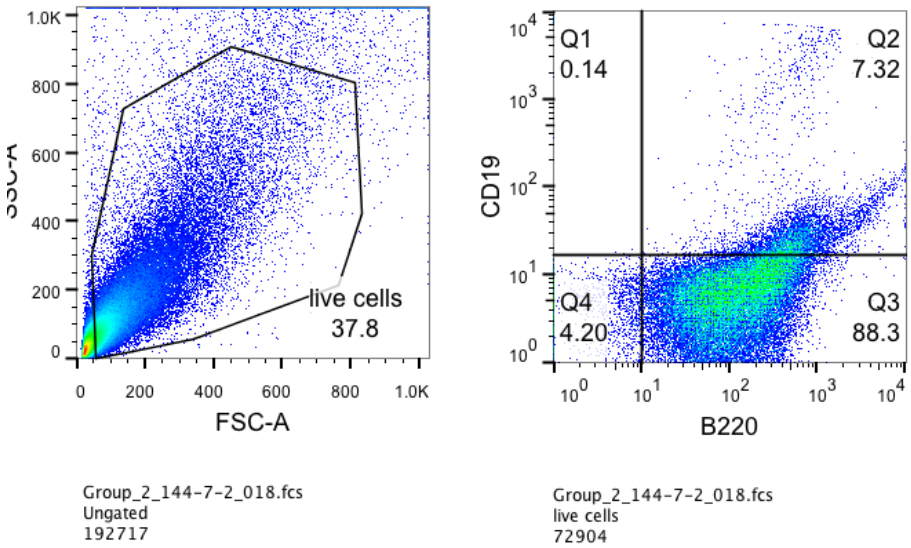

B.

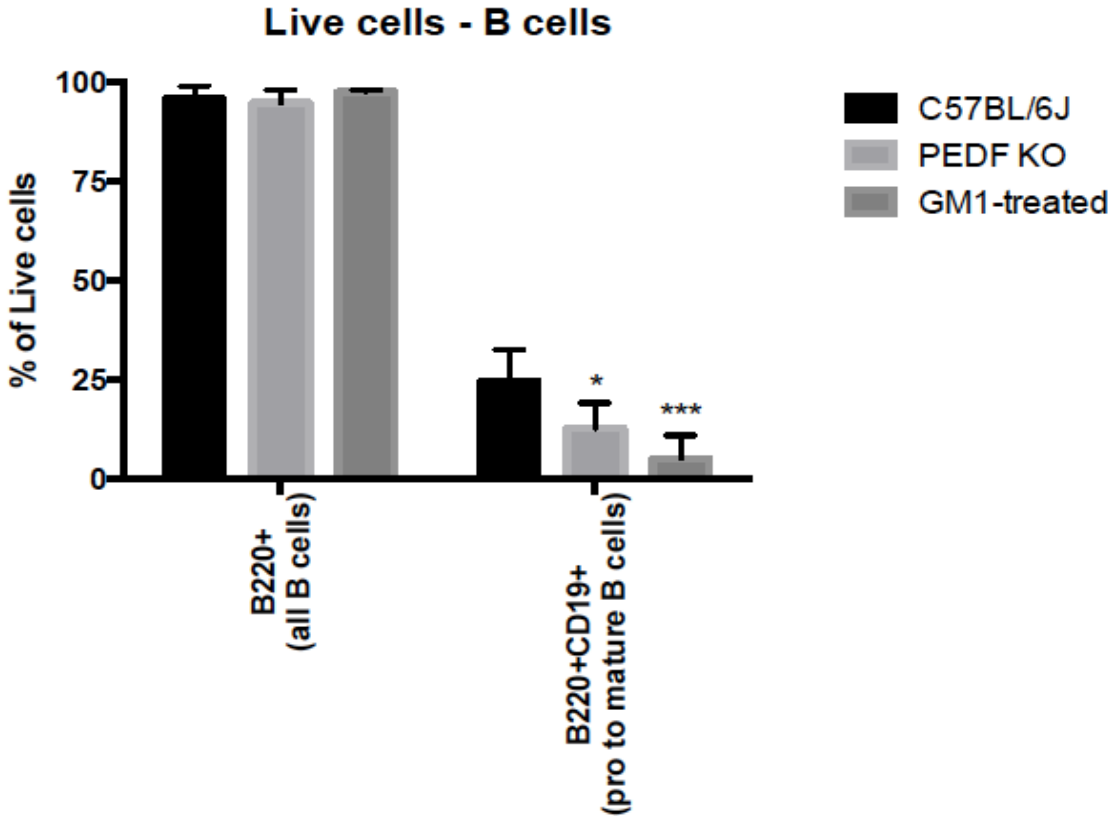

Figure 13. FACS analysis revealed a statistically significant decrease in mature B cells in the livers of PEDF KO mice and GM1 treated mice. A. Representative images of FACS analysis of B220+ cells divided based on their expression of CD19. **B.** The bar graph shows the results of the FACS analysis. Both PEDF KO, and NK cell deficient mice showed a statistically significant decrease in the percentage of mature B cells. Data are reported with standard error of the mean, *p<.05, ***p<.001, n=3, using multiple t-tests (Morales, unpublished).

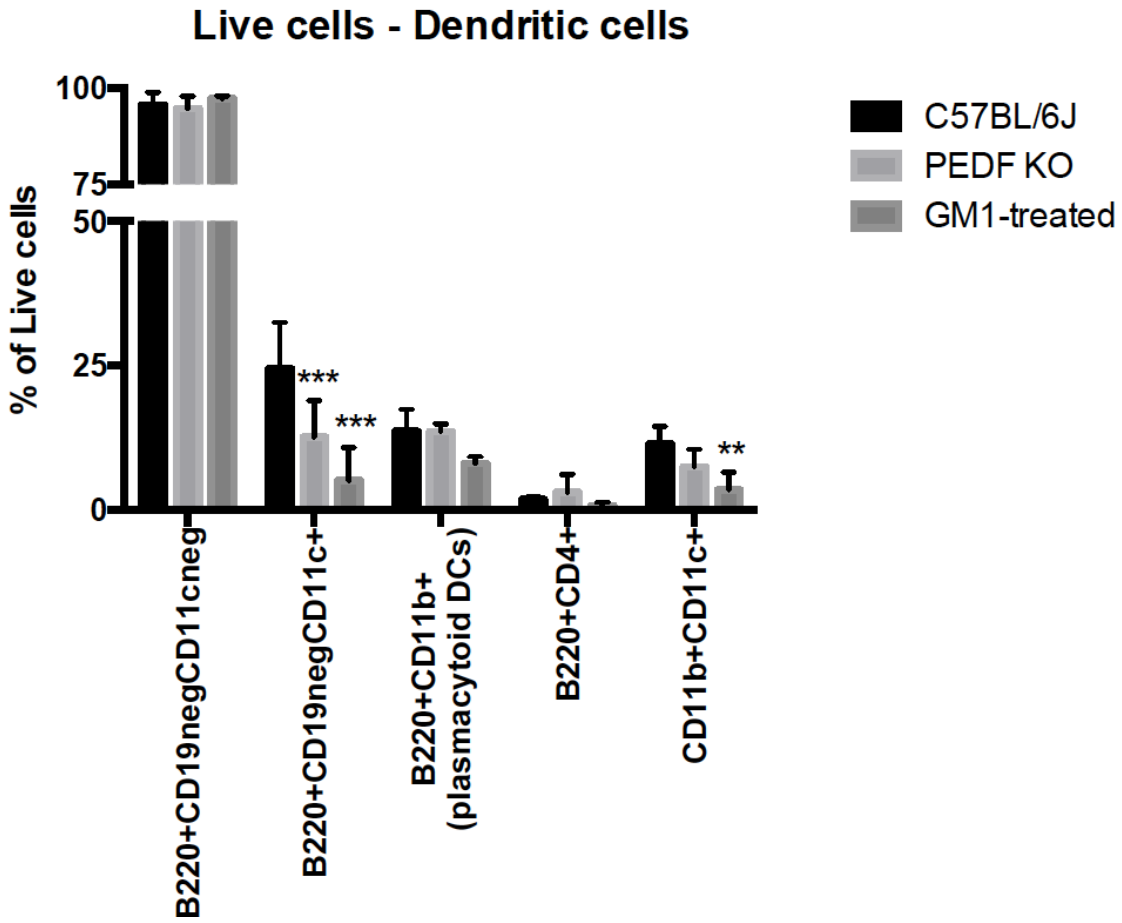

Figure 14. FACS analysis shows significant decrease in CD11c+ expressing mature dendritic cells in the livers of PEDF KO mice and GM1 treated mice. Four distinct populations of B220+CD19neg cells, B220+ CD19neg CD11c+, B220+CD11b+, B220+CD4+, and CD11b+ CD11c+, were examined. The bar graph shows the cumulative results of FACS analysis of the four subsets of myeloid derived cells. PEDF KO mice and GM1 treated mice had a statistically significant decrease in the percentage of mature dendritic cells. GM1 treated mice had a significant decrease in CD11b+CD11c+ expressing cells. Data are reported with standard error of the mean, **p<.01, ***p<.001, n=3, using multiple t-tests (Morales, unpublished).

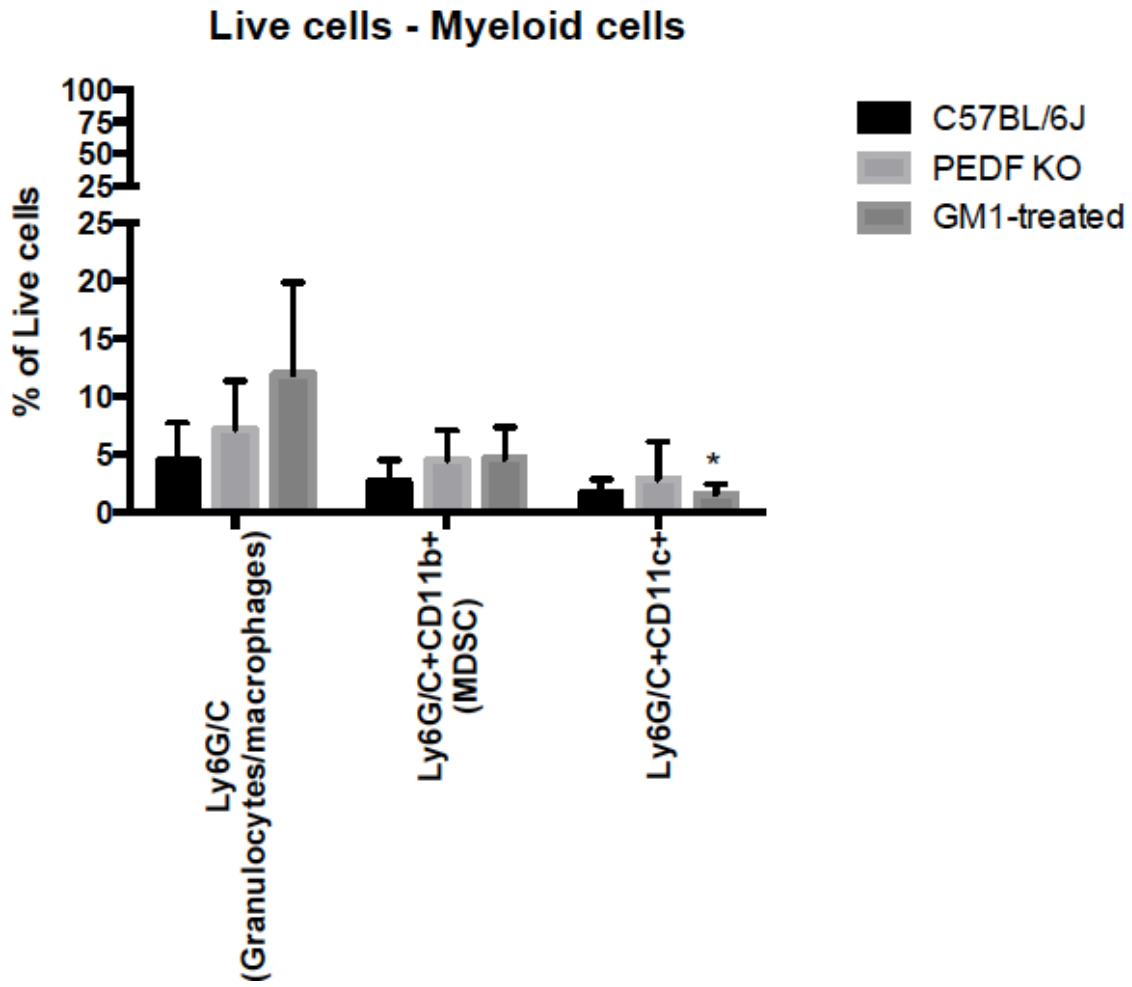

Figure 15. FACS analysis showed an increase in myeloid derived suppressor cells in PEDF KO and GM1 treated mice. MDSCs are Ly6G/C+CD11b+ expressing cells. Although results are not statistically significant there was slight increase in MDSCs in PEDF KO and GM1 treated mice. Data are reported with standard error of the mean, *p<.05, n=3, using multiple t-tests (Morales, unpublished).

Discussion

In support of our initial hypothesis wild-type mice developed an equal distribution of metastases in the infiltrative and nodular pattern of growth. Wild-type mice predominantly developed stage 1 micrometastases, and a few avascular stage 2 metastases. In comparison to wild-type mice, PEDF KO mice showed a statistically significant increase in the number of metastases in the nodular pattern of growth. In addition, PEDF KO mice had a greater number of stage 2 and stage 3 metastases in comparison to wild-type mice. Research has shown that PEDF produced by hepatocytes is important in suppressing metastatic progression by inhibiting angiogenesis and stromagenesis within metastases. PEDF inhibits the angiogenic properties of VEGF by inducing apoptosis in endothelial cells and HSCs. However, melanoma cells have developed means to suppress PEDF in metastatic tissue. In hypoxic conditions, melanoma cells and macrophages secrete MMP-2 and MMP-9 which degrade host PEDF produced by hepatocytes. These findings suggest that as tumors increase in size they are able to downregulate PEDF and shift the VEGF: PEDF ratio toward VEGF production.

There is increasing evidence of the protective function of PEDF in inhibiting metastatic progression, however the contribution of stromal PEDF, derived from cancer associated fibroblasts, is not well understood. Cancer associated fibroblasts compose a significant portion of the tumor microenvironment (Kalluri and Zeisberg 2006, Nwani et al. 2016). Crosstalk between tumor cells and host stromal cells causes host cells to assume cancer associated properties that support tumor growth (Tlsty and Hein 2001, Nwani et al. 2016). Fibroblasts that express PEDF are able to

inhibit metastatic progression. Yet, recent studies have shown that PEDF null melanoma cells suppress PEDF expression in fibroblasts in close contact. These melanoma cells produce PDGF-BB (platelet-derived growth factor BB) and TGFβ which block PEDF production in cancer associated fibroblasts and in turn diminish their tumor suppressive properties (Nwani et al. 2016). This mechanism suggests that in the livers of mice expressing PEDF, melanoma cells may downregulate PEDF expression in the surrounding stroma diminishing PEDF-mediated inhibition of tumor progression. This finding potentially explains how tumors in the nodular pattern of growth are able to establish metastases and proliferate in the PEDF competent livers. In future experiments, further investigation into fibroblast expression of PEDF would elucidate the contribution of stromal PEDF in tumorigenesis.

A parallel hypothesis is that both peripheral blood natural killer cells and intrinsic hepatic natural killer cells protect the periportal area and sinusoidal space. Contrary to the original hypothesis, NK cell deficient mice showed increased stage 2 infiltrative and nodular metastases which shows that NK cell deficiency lead to increased metastatic progression of tumors in both patterns. NK cell deficient mice also presented with an increased number of hepatic metastasis relative to PEDF KO and wild type mice. Some metastases were grossly visible and NK cell deficient mice had an increased number of stage 3 metastases in comparison to wild type mice. From this data we hypothesize that there are two ways the tumor can be exposed to the host immune response, and more specifically that infiltrating natural killer cells from the periphery are protecting the periportal area.

For this experiment we previously assumed that the periportal area was an immune privileged site. Peripheral blood (PB) NK cells can be recruited from the blood to local sites of inflammation in tissue (Hudspeth et al. 2013). NK cells are important effectors of the innate immune response, and hepatic-NK cells account for 50% of the total liver lymphocyte population. Liver macrophages, or Kupffer cells, coordinate the immune response, by acting as regulatory cells that can amplify immune response by producing cytokines and chemokines (Hudspeth et al. 2013). Our data showed statistically significant increase in the number of stage 2 metastases, this increase may be due to disruption of the paracrine and autocrine loops coordinating immune response following loss of NK cell function. Mice were sacrificed 3 weeks after inoculation with tumor cells. Based on the collected data, mice in the PEDF KO and anti-asialo GM1 treated group would likely have significantly more stage 3 metastases if they were allowed to live longer. Especially, in the GM1 treated group because these mice presented grossly visible metastases 3 weeks after inoculation.

Hepatic-NK cells also have enhanced cytolytic potential over PB-NK cells, which indicate that they likely serve as sentinels in the liver. Hepatic-NK cells are able to lyse cell lines that are resistant to PB-NK cell cytolysis (Hudspeth et al. 2013). The enhanced cytolytic activity of hepatic NK cells may explain why these cells have a more potent effect in the sinusoidal spaces, validated by the reduced number of stage 2 and stage 3 metastases in sinusoidal spaces of PEDF KO and wild-type mice. Also, this mechanism suggests that PB-NK cells may be working in conjunction with PEDF to suppress metastasis in the periportal area. PB-NK cells

and PEDF both have antagonistic effects on cells in the nodular pattern, which could explain the reduction in stage 2 and stage 3 metastases in wild-type mice. Further experimentation with immunostaining for lymphocyte infiltration would be crucial in understanding the role of NK cells in the immune response to tumor cells.

Previous experiments using the TLR-5 agonist Entolimod, and interferon-α2b reduced the number of hepatic metastases. Mice treated with entolimod injections had significant reduction in the number of metastatic nodules in the liver. The mechanism of action behind entolimod's antimetastatic effect is increased homing of blood borne NK cells, maturation and activation in the liver (Yang et al. 2016). Similarly, as previously demonstrated in Figure 3, injections of IFN- α2b enhances the activity of IFN- γ expressing NK cells further potentiating hepatic NK cell activity (Yang et al. 2004). These data again suggest that PB-NK cells and hepatic-NK cells are crucial components of the innate immune response to tumor cells in the liver.

Although NK cells are depleted in the NK cell deficient mouse, we hypothesized that this would not affect other lymphocytes that may have an anti-melanoma effect. However, FACS analysis revealed a significant reduction in the number of mature B cells which possibly suggests that immune suppression in the tumor microenvironment is required for metastatic progression of uveal melanoma. In addition to NK cell deficiency, increased tumor burden may further immunosuppression by upregulating MDSC activation thus reducing CD8+ T cell and NK cell cytotoxicity. Further investigation of B cell populations revealed that PEDF

KO and NK cell deficient mice showed a statistically significant decrease in CD11c+ expressing mature dendritic cells. CD11c- cells represent a subpopulation of immature dendritic cells referred to as pre-plasmacytoid dendritic cells, immediate precursors of plasmacytoid dendritic cells. Plasmacytoid dendritic cells are responsible for initiating host innate and adaptive immune responses, which results in indirect/direct activation of monocytes, mature dendritic cells, B cells, NK cells, and T cells (McKenna et al. 2005).

The tumor cells are able to communicate with the host microenvironment to induce an immunosuppressive state that promotes tumor progression and reduces T cell cytotoxicity (Ostrand-Rosenberg et al. 2012). Myeloid-derived suppressor cell activity is heightened in most malignancies. MDSCs inhibit adaptive and innate immunity through multiple mechanisms that directly affect CD4+ and CD8+ T cells, NK cells, and NK cell production of IFNγ (Ostrand-Rosenberg et al. 2012). MDSCs are recruited to the tumor site by a variety of tumor-derived soluble factors that affect myelopoiesis, myeloid cell mobilization, and activation (Dolcetti et al. 2008).

Defective dendritic cell function is also a commonality in patients with malignancies. Dendritic cells function as antigen presenting cells that prime the immune T cell response. Tumor cells are able to disrupt this system to enhance tumor growth by increasing the number of immature dendritic cells and decreasing the number of mature dendritic cells (Gabrilovich 2004, Ostrand-Rosenberg et al. 2012). MDSC-DC crosstalk may be responsible for dendritic cell dysfunction (Sinha et al. 2007, Ostrand-Rosenberg et al. 2012). Studies with melanoma cells

demonstrate that MDSCs are able to impair DC maturation by reducing antigen uptake, prevent migration of innate and mature dendritic cells, and block the ability of dendritic cells to induce IFNγ-producing T cells (Ostrand-Rosenberg et al. 2012, Poschke et al. 2012). Tumor associated dendritic cells produce IL-23 and induce TH17 cells which contribute to the effects of MDSCs. IL-23 production also fuels tumor progression by driving TH17 cells which suppress adaptive and innate immunity **(Figure 16)** (Ostrand-Rosenberg et al. 2012). This mechanism exemplifies that tumor cells are able to communicate with cells of the microenvironment and induce a pro-metastatic environment.

It is important to determine if tumor burden is suppressing B cell maturation, and negate the possibility that PEDF and anti-asialo GM1 have an effect on B cell maturation. Current research reveals no direct link between PEDF and B cells, however, studies have shown that PEDF is an endogenous anti-inflammatory molecule (Zhang et al. 2006). Further investigation of the mechanism is important to determine if uveal melanoma cells are able to suppress the B cell mediated immune response, which may have an impact on immune therapy.

In summary, we found that knockout of PEDF in mice leads to increased nodular pattern, which shows that PEDF has a distinct role in preventing metastatic progression of tumors in the periportal area. Depletion of NK cells leads to an increased number of hepatic metastases and increased stage 2 metastases of both nodular and infiltrative pattern. This data suggests that NK cells infiltrate both the periportal area and sinusoidal spaces and protect these compartments from

metastasis. FACS analysis of liver lymphocyte populations revealed significant reduction in mature B cells. We hypothesize that increased tumor burden, facilitated by loss of protective mechanisms, initiates dendritic cell dysfunction and upregulation of MDSCs that results in an immunosuppressive tumor microenvironment. We propose a new mechanism in which uveal melanoma cells are able to inhibit host PEDF and suppress the immune response in the tumor microenvironment **(Figure 17).** In hypoxic conditions, melanoma cells degrade host PEDF by producing MMP-2 and MMP-9. They also inhibit fibroblast-derived PEDF in tumor associated fibroblasts through PDGF-BB and TGFβ. Hepatic and peripheral blood NK cells normally function to protect the periportal area and sinusoidal space from metastasis. However, as tumor burden increases, melanoma cells recruit MDSCs and tumor associated dendritic cells which in turn suppresses cytotoxic T cell and NK cell activity, and also decreases dendritic cell maturation and antigen uptake. Combined disruption of PEDF and NK cells protective effects, by melanoma cells, allows for metastatic progression of tumors in the periportal area and sinusoidal space.

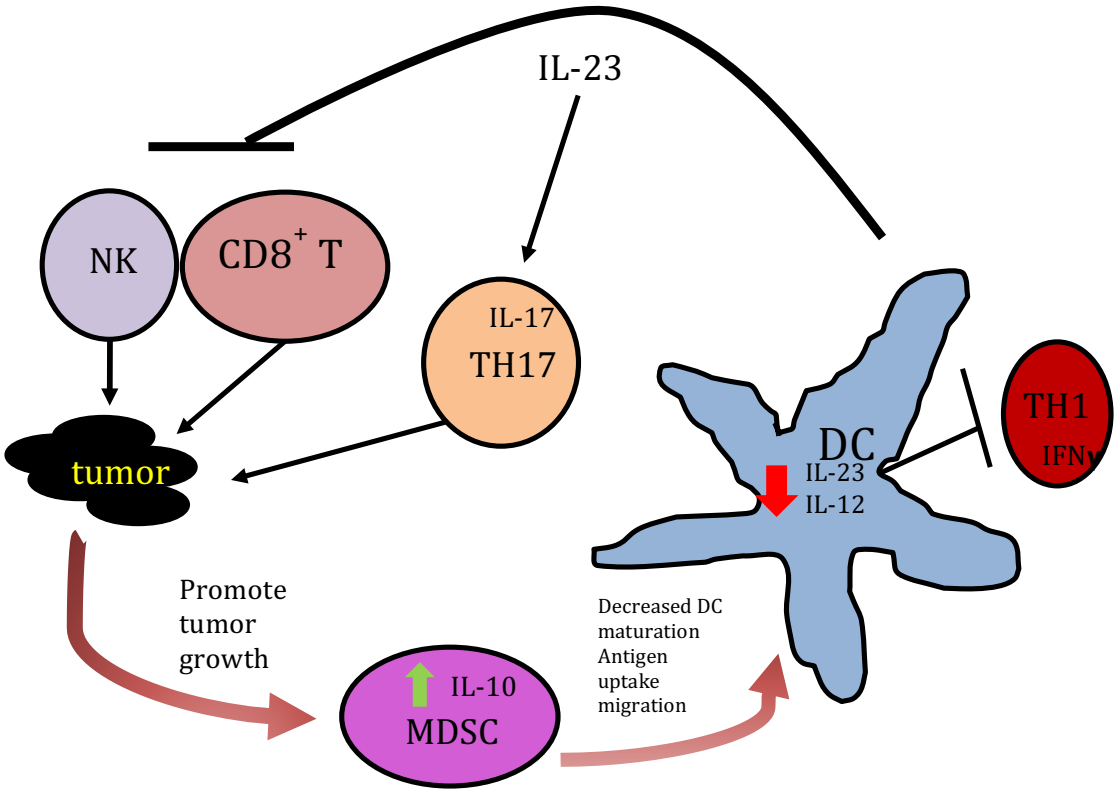

Figure 15. Increased tumor burden induces dendritic cell dysfunction and MDSC activation. Cross-talk between MDSC and tumor associated dendritic cells promotes metastatic progression of tumor cells. Tumor associated dendritic cells promote tumor growth by producing IL-23 which suppresses T cell and NK cell cytotoxicity. IL-23 also stimulates TH17 cells that produce IL-17 which further supports tumor progression. Increased tumor burden upregulates activation of MDSCs which decrease DC maturation, antigen uptake, migration, IL-23, IL-12, and T cell production of IFNγ. MDSC accumulation further limits activation of the CD8-mediated anti-tumor immunity thus facilitating tumor progression (Ostrand-Rosenberg et al. 2012).

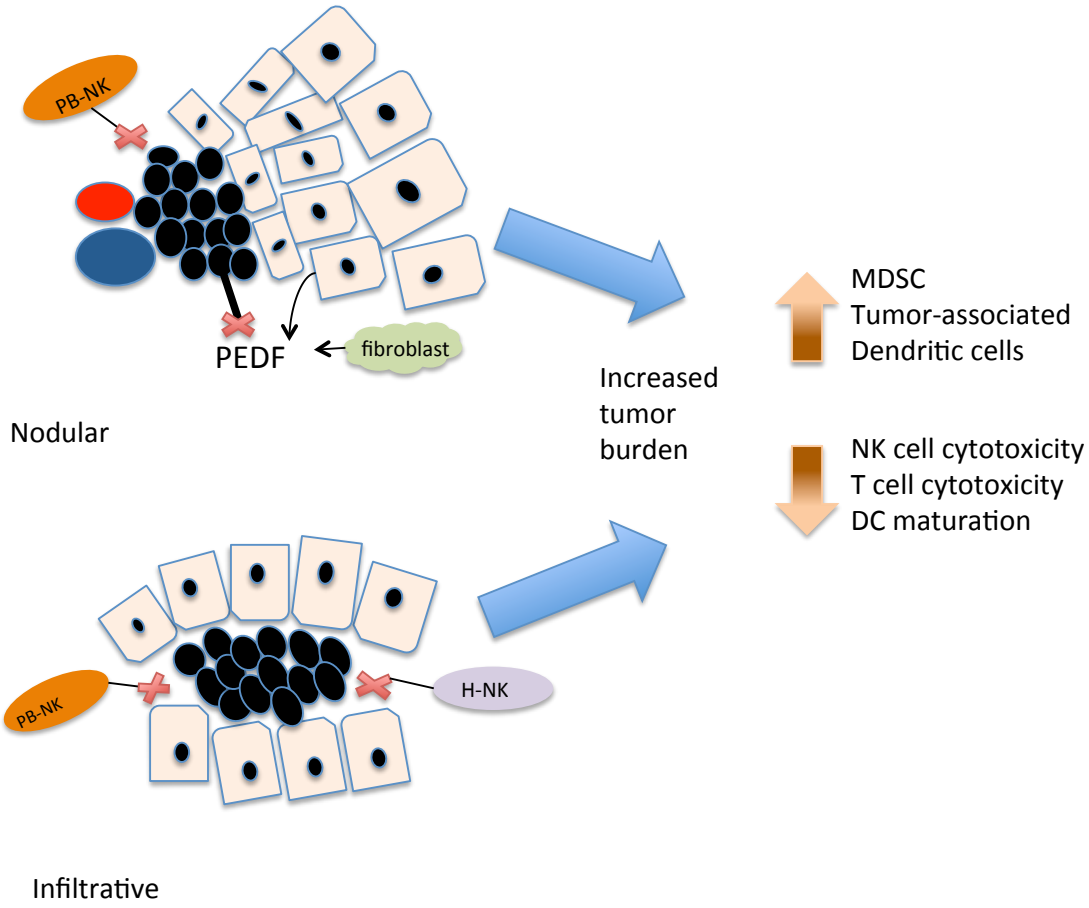

Figure 17. Melanoma cells inhibit host PEDF and suppress the immune response to promote metastatic progression in the liver. In normal liver host PEDF and NK cells protect the periportal area and sinusoidal spaces from metastasis. However once uveal melanoma become established in the liver, melanoma cells secrete MMP-2 and MMP-9 to degrade host PEDF produced by hepatocytes. Melanoma cells recruit fibroblasts to support metastatic growth. The tumor cells inhibit fibroblast derived PEDF through PDGF-BB and TGFβ. As tumor burden increases, the melanoma cells upregulate MDSCs and tumor associated dendritic cells. MDSCs and tumor-associated dendritic cells function to support tumor growth, and suppress the immune response by downregulating T cell and NK cell cytotoxicity, and by reducing dendritic cell maturation and antigen uptake.

References

Abdel-Rahman, M. H., C. M. Cebulla, V. Verma, B. N. Christopher, W. E. Carson, 3rd, T. Olencki and F. H. Davidorf (2012). "Monosomy 3 status of uveal melanoma metastases is associated with rapidly progressive tumors and short survival." Exp Eye Res **100**: 26-31.

Albert, D. M., L. M. Ryan and E. C. Borden (1996). "Metastatic ocular and cutaneous melanoma: a comparison of patient characteristics and prognosis." Arch Ophthalmol **114**(1): 107-108.

Asnaghi, L., G. Gezgin, A. Tripathy, J. T. Handa, S. L. Merbs, P. A. van der Velden, M. J. Jager, J. W. Harbour and C. G. Eberhart (2015). "EMT-associated factors promote invasive properties of uveal melanoma cells." Mol Vis **21**: 919-929.

Bakalian, S., J. C. Marshall, P. Logan, D. Faingold, S. Maloney, S. Di Cesare, C. Martins, B. F. Fernandes and M. N. Burnier, Jr. (2008). "Molecular pathways mediating liver metastasis in patients with uveal melanoma." Clin Cancer Res **14**(4): 951-956.

Blom, D. J., G. P. Luyten, C. Mooy, S. Kerkvliet, A. H. Zwinderman and M. J. Jager (1997). "Human leukocyte antigen class I expression. Marker of poor prognosis in uveal melanoma." Invest Ophthalmol Vis Sci **38**(9): 1865-1872.

Cai, J., W. G. Jiang, M. B. Grant and M. Boulton (2006). "Pigment epithelium-derived factor inhibits angiogenesis via regulated intracellular proteolysis of vascular endothelial growth factor receptor 1." J Biol Chem **281**(6): 3604-3613.

Cantore, M., G. Fiorentini, E. Aitini, B. Davitti, G. Cavazzini, C. Rabbi, A. Lusenti, M. Bertani, C. Morandi, V. Benedini and et al. (1994). "Intra-arterial hepatic carboplatin-based chemotherapy for ocular melanoma metastatic to the liver. Report of a phase II study." Tumori **80**(1): 37-39.

Chen, L., S. S. Zhang, C. J. Barnstable and J. Tombran-Tink (2006). "PEDF induces apoptosis in human endothelial cells by activating p38 MAP kinase dependent cleavage of multiple caspases." Biochem Biophys Res Commun **348**(4): 1288-1295.

Damato, E. M. and B. E. Damato (2012). "Detection and time to treatment of uveal melanoma in the United Kingdom: an evaluation of 2,384 patients." Ophthalmology **119**(8): 1582-1589.

Dawson, D. W., O. V. Volpert, P. Gillis, S. E. Crawford, H. Xu, W. Benedict and N. P. Bouck (1999). "Pigment epithelium-derived factor: a potent inhibitor of angiogenesis." Science **285**(5425): 245-248.

Diaz, C. E., D. Rusciano, S. Dithmar and H. E. Grossniklaus (1999). "B16LS9 melanoma cells spread to the liver from the murine ocular posterior compartment (PC)." Curr Eye Res **18**(2): 125-129.

Dithmar, S. A., D. A. Rusciano, C. A. Armstrong, M. J. Lynn and H. E. Grossniklaus (1999). "Depletion of NK cell activity results in growth of hepatic micrometastases in a murine ocular melanoma model." Curr Eye Res **19**(5): 426-431.

Dolcetti, L., I. Marigo, B. Mantelli, E. Peranzoni, P. Zanovello and V. Bronte (2008). "Myeloid-derived suppressor cell role in tumor-related inflammation." Cancer Lett **267**(2): 216-225.

Eagle, R. C., Jr. (2013). "The pathology of ocular cancer." Eye (Lond) **27**(2): 128-136.

eBioscience, A. "Anti-Asialo-GM1 Functional Grade Purified." 2016, from http://www.ebioscience.com/asialo-gm-1-antibody-fg-purified.htm.

Fernandez-Barral, A., J. L. Orgaz, V. Gomez, L. del Peso, M. J. Calzada and B. Jimenez (2012). "Hypoxia negatively regulates antimetastatic PEDF in melanoma cells by a hypoxia inducible factor-independent, autophagy dependent mechanism." PLoS One **7**(3): e32989.

Gabrilovich, D. (2004). "Mechanisms and functional significance of tumour-induced dendritic-cell defects." Nat Rev Immunol **4**(12): 941-952.

Gamel, J. W., I. W. McLean, R. A. Greenberg, L. E. Zimmerman and S. J. Lichtenstein (1982). "Computerized histologic assessment of malignant potential: a method for determining the prognosis of uveal melanomas." Hum Pathol **13**(10): 893-897.

Grossniklaus, H. E. (2013). "Progression of ocular melanoma metastasis to the liver: the 2012 Zimmerman lecture." JAMA Ophthalmol **131**(4): 462-469.

Grossniklaus, H. E., Q. Zhang, H. Yang, Y. Shou, S. Kang and J. M. Lattier (2014). Progression of Ocular Melanoma Metastasis to the Liver in Mouse Model. ARVO Annual Meeting, Investigative Opthalmology and Visual Science.

Habu, S., H. Fukui, K. Shimamura, M. Kasai, Y. Nagai, K. Okumura and N. Tamaoki (1981). "In vivo effects of anti-asialo GM1. I. Reduction of NK activity and enhancement of transplanted tumor growth in nude mice." J Immunol **127**(1): 34-38.

Hans-Gustaf, L. a. K. K. (1990). "In search of the 'missing self': MHC molecules and NK cell recognition." Immunology Today **11**(7): 237-244.

Harbour, J. W., M. D. Onken, E. D. Roberson, S. Duan, L. Cao, L. A. Worley, M. L. Council, K. A. Matatall, C. Helms and A. M. Bowcock (2010). "Frequent mutation of BAP1 in metastasizing uveal melanomas." Science **330**(6009): 1410-1413.

Harning, R., G. C. Koo and J. Szalay (1989). "Regulation of the metastasis of murine ocular melanoma by natural killer cells." Invest Ophthalmol Vis Sci **30**(9): 1909-1915.

Hicklin, D. J. and L. M. Ellis (2005). "Role of the vascular endothelial growth factor pathway in tumor growth and angiogenesis." J Clin Oncol **23**(5): 1011-1027.

Ho, T. C., S. L. Chen, S. C. Shih, J. Y. Wu, W. H. Han, H. C. Cheng, S. L. Yang and Y. P. Tsao (2010). "Pigment epithelium-derived factor is an intrinsic antifibrosis factor targeting hepatic stellate cells." Am J Pathol **177**(4): 1798-1811.

Hu, D. N., J. D. Simon and T. Sarna (2008). "Role of ocular melanin in ophthalmic physiology and pathology." Photochem Photobiol **84**(3): 639-644.

Hudspeth, K., E. Pontarini, P. Tentorio, M. Cimino, M. Donadon, G. Torzilli, E. Lugli, S. Della Bella, M. E. Gershwin and D. Mavilio (2013). "The role of natural killer cells in autoimmune liver disease: a comprehensive review." J Autoimmun **46**: 55-65.

Kalluri, R. and M. Zeisberg (2006). "Fibroblasts in cancer." Nat Rev Cancer **6**(5): 392-401.

Landreville, S., O. A. Agapova and J. W. Harbour (2008). "Emerging insights into the molecular pathogenesis of uveal melanoma." Future Oncol **4**(5): 629-636.

Lattier, J. M., H. Yang, S. Crawford and H. E. Grossniklaus (2013). "Host pigment epithelium-derived factor (PEDF) prevents progression of liver metastasis in a mouse model of uveal melanoma." Clin Exp Metastasis **30**(8): 969-976.

Lu, X. and Y. Kang (2010). "Hypoxia and hypoxia-inducible factors: master regulators of metastasis." Clin Cancer Res **16**(24): 5928-5935.

Ma, D., G. P. Luyten, T. M. Luider and J. Y. Niederkorn (1995). "Relationship between natural killer cell susceptibility and metastasis of human uveal melanoma cells in a murine model." Invest Ophthalmol Vis Sci **36**(2): 435-441.

Mallikarjuna, K., V. Pushparaj, J. Biswas and S. Krishnakumar (2007). "Expression of epidermal growth factor receptor, ezrin, hepatocyte growth factor, and c-Met in uveal melanoma: an immunohistochemical study." Curr Eye Res **32**(3): 281-290.

Materin, M. A. D., B. (2011). "Uveal Melanoma--Where Are We Going?" US Opthalmic Review **4**(1): 105-107.

McKenna, K., A. S. Beignon and N. Bhardwaj (2005). "Plasmacytoid dendritic cells: linking innate and adaptive immunity." J Virol **79**(1): 17-27.

McKinnon, J. G., X. Q. Yu, W. H. McCarthy and J. F. Thompson (2003). "Prognosis for patients with thin cutaneous melanoma: long-term survival data from New South Wales Central Cancer Registry and the Sydney Melanoma Unit." Cancer **98**(6): 1223-1231.

Miyamoto, C., M. Balazsi, S. Bakalian, B. F. Fernandes and M. N. Burnier, Jr. (2012). "Uveal melanoma: Ocular and systemic disease." Saudi J Ophthalmol **26**(2): 145-149.

Notari, L., N. Arakaki, D. Mueller, S. Meier, J. Amaral and S. P. Becerra (2010). "Pigment epithelium-derived factor binds to cell-surface F(1)-ATP synthase." FEBS J **277**(9): 2192-2205.

Nwani, N. G., M. L. Deguiz, B. Jimenez, E. Vinokour, O. Dubrovskyi, A. Ugolkov, A. P. Mazar and O. V. Volpert (2016). "Melanoma Cells Block PEDF Production in Fibroblasts to Induce the Tumor-Promoting Phenotype of Cancer-Associated Fibroblasts." Cancer Res **76**(8): 2265-2276.

Onken, M. D., J. P. Ehlers, L. A. Worley, J. Makita, Y. Yokota and J. W. Harbour (2006). "Functional gene expression analysis uncovers phenotypic switch in aggressive uveal melanomas." Cancer Res **66**(9): 4602-4609.

Onken, M. D., L. A. Worley, J. P. Ehlers and J. W. Harbour (2004). "Gene expression profiling in uveal melanoma reveals two molecular classes and predicts metastatic death." Cancer Res **64**(20): 7205-7209.

Ostrand-Rosenberg, S., P. Sinha, D. W. Beury and V. K. Clements (2012). "Cross-talk between myeloid-derived suppressor cells (MDSC), macrophages, and dendritic cells enhances tumor-induced immune suppression." Semin Cancer Biol **22**(4): 275-281.

Pina, Y., C. M. Cebulla, T. G. Murray, A. Alegret, S. R. Dubovy, H. Boutrid, W. Feuer, L. Mutapcic and M. E. Jockovich (2009). "Blood vessel maturation in human

uveal melanoma: spatial distribution of neovessels and mature vasculature." Ophthalmic Res **41**(3): 160-169.

Poschke, I., Y. Mao, L. Adamson, F. Salazar-Onfray, G. Masucci and R. Kiessling (2012). "Myeloid-derived suppressor cells impair the quality of dendritic cell vaccines." Cancer Immunol Immunother **61**(6): 827-838.

Singh, A. D., M. E. Turell and A. K. Topham (2011). "Uveal melanoma: trends in incidence, treatment, and survival." Ophthalmology **118**(9): 1881-1885.

Sinha, P., V. K. Clements, A. M. Fulton and S. Ostrand-Rosenberg (2007). "Prostaglandin E2 promotes tumor progression by inducing myeloid-derived suppressor cells." Cancer Res **67**(9): 4507-4513.

Tlsty, T. D. and P. W. Hein (2001). "Know thy neighbor: stromal cells can contribute oncogenic signals." Curr Opin Genet Dev **11**(1): 54-59.

Van den Eynden, G. G., A. W. Majeed, M. Illemann, P. B. Vermeulen, N. C. Bird, G. Hoyer-Hansen, R. L. Eefsen, A. R. Reynolds and P. Brodt (2013). "The multifaceted role of the microenvironment in liver metastasis: biology and clinical implications." Cancer Res **73**(7): 2031-2043.

Van Raamsdonk, C. D., V. Bezrookove, G. Green, J. Bauer, L. Gaugler, J. M. O'Brien, E. M. Simpson, G. S. Barsh and B. C. Bastian (2009). "Frequent somatic mutations of GNAQ in uveal melanoma and blue naevi." Nature **457**(7229): 599-602.

Vidal-Vanaclocha, F. (2008). "The prometastatic microenvironment of the liver." Cancer Microenviron **1**(1): 113-129.

Volpert, O. V., T. Zaichuk, W. Zhou, F. Reiher, T. A. Ferguson, P. M. Stuart, M. Amin and N. P. Bouck (2002). "Inducer-stimulated Fas targets activated endothelium for destruction by anti-angiogenic thrombospondin-1 and pigment epithelium-derived factor." Nat Med **8**(4): 349-357.

Woll, E., A. Bedikian and S. S. Legha (1999). "Uveal melanoma: natural history and treatment options for metastatic disease." Melanoma Res **9**(6): 575-581.

Woodward, J. K., S. R. Elshaw, A. K. Murray, C. E. Nichols, N. Cross, D. Laws, I. G. Rennie and K. Sisley (2002). "Stimulation and inhibition of uveal melanoma invasion by HGF, GRO, IL-1alpha and TGF-beta." Invest Ophthalmol Vis Sci **43**(10): 3144-3152.

Xu, X., W. B. Wei, B. Li, F. Gao, Z. Zhang and J. B. Jonas (2014). "Oncogenic GNAQ and GNA11 mutations in uveal melanoma in Chinese." PLoS One **9**(10): e109699.

Yang, H., C. M. Brackett, V. M. Morales-Tirado, Z. Li, Q. Zhang, M. W. Wilson, C. Benjamin, W. Harris, E. K. Waller, A. V. Gudkov, L. G. Burdelya and H. E. Grossniklaus (2016). "The Toll-like receptor 5 agonist entolimod suppresses hepatic metastases in a murine model of ocular melanoma via an NK cell-dependent mechanism." Oncotarget **7**(3): 2936-2950.

Yang, H., S. Dithmar and H. E. Grossniklaus (2004). "Interferon alpha 2b decreases hepatic micrometastasis in a murine model of ocular melanoma by activation of intrinsic hepatic natural killer cells." Invest Ophthalmol Vis Sci **45**(7): 2056-2064.

Yang, H., M. J. Jager and H. E. Grossniklaus (2010). "Bevacizumab suppression of establishment of micrometastases in experimental ocular melanoma." Invest Ophthalmol Vis Sci **51**(6): 2835-2842.

Yang, H., Z. Xu, P. M. Iuvone and H. E. Grossniklaus (2006). "Angiostatin decreases cell migration and vascular endothelium growth factor (VEGF) to pigment epithelium derived factor (PEDF) RNA ratio in vitro and in a murine ocular melanoma model." Mol Vis **12**: 511-517.

Zhang, S. X., J. J. Wang, G. Gao, K. Parke and J. X. Ma (2006). "Pigment epithelium-derived factor downregulates vascular endothelial growth factor (VEGF) expression and inhibits VEGF-VEGF receptor 2 binding in diabetic retinopathy." J Mol Endocrinol **37**(1): 1-12.

Zhang, S. X., J. J. Wang, G. Gao, C. Shao, R. Mott and J. X. Ma (2006). "Pigment epithelium-derived factor (PEDF) is an endogenous antiinflammatory factor." FASEB J **20**(2): 323-325.